5.1 Preformulation studies

5.1.1 UV Spectrophotometric analysis

5.1.1.1 Standard calibration curve

The analytical method based on UV-visible spectrophotometry was developed for quantitative estimation of docetaxel in acetonitrile and pH 7.4 saline phosphate buffer (70:30). A stock solution of docetaxel (100 µg/mL) was prepared and serially diluted to give a range of standard concentrations. From the standard stock solution, set of dilutions were prepared to get concentration range of 5, 10, 15, 20, 25, 30, 35, 40, 45 and 50 µg/mL with the help of specific solvent and absorbance was taken at 231 nm (Table 5.1). UV-Visible spectrophotometer was used for plotting a calibration curve of docetaxel in the concentration range of 5-50 µg/mL, and slopes with regression coefficient were obtained (Figure 5.1). The amount or concentration of docetaxel was estimated using its standard calibration curve.

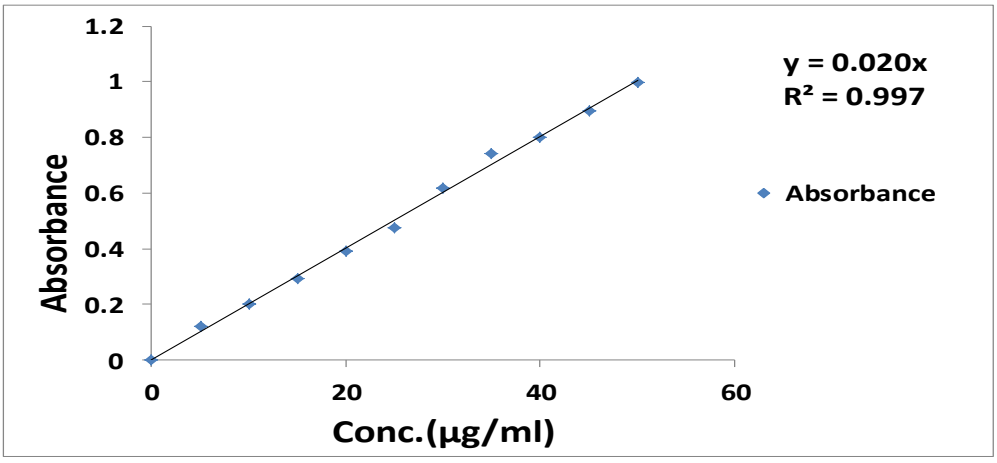

Figure 5.1 Calibration curve of docetaxel in acetonitrile and pH 7.4 saline phosphate buffer (70:30) at 231 nm

Table 5.1 Absorbance data for calibration curve of docetaxel

Concentration (µg/mL)	Absorbance		
	Absorbance*	± SD	% RSD
0	0	0	0
5	0.121	0.0018	1.4876
10	0.200	0.0025	1.2500
15	0.292	0.0020	0.6849
20	0.390	0.0010	0.2564
25	0.476	0.0043	0.9033
30	0.617	0.0100	1.6207
35	0..741	0.0037	0.4993
40	0.801	0.0082	1.0237
45	0.894	0.0059	0.6599
50	0.997	0.0034	0.3410

***Average of three determinations**

Inference

Standard plot of docetaxel in acetonitrile and pH 7.4 saline phosphate buffer (70:30) was found to be linear (straight line) with R^2 value 0.997, showed a proportional increase in the absorbance with concentration.

5.1.2 HPLC analytical method development and validation

5.1.2.1 Method development

Method development was performed to optimize the compositional factors to meet the requirements for the intended analytical applications using the Box-Behnken design for experimentation. The design which was generated encompassed the entire knowledge space defined by the response constraint, and independent variables entered during the experimental setup (Table 5.2). This demonstrated an analytical procedure which accurately and precisely predicts the concentration of unknown samples.

Table 5.2 Box-Behnken Design with 17 experimental runs and their measured responses

Run	Factor 1 (A) A: Column Temp.	Factor 2 (B) B: Flow Rate	Factor 3 (C) C: % Org Phase	Response (Y) T. Plate*
1	0	0	0	16974.3±3.220
2	1	-1	0	17409.5±5.031
3	0	1	-1	17534.8±2.072
4	-1	1	0	17209.6±7.1
5	0	-1	1	17035.2±12.065
6	-1	0	-1	17182.4±6.072
7	1	0	1	17334.3±2.1
8	-1	-1	0	16886.7±9.081
9	0	0	0	16900.3±10.064
10	1	0	-1	17503.3±1.097
11	0	0	0	16925.4±3.031
12	1	1	0	17536.9±13.023
13	0	0	0	16834.1±4.091
14	0	0	0	16821.4±9.042
15	0	-1	-1	17102.7±8.087
16	0	1	1	17253.2±6.012
17	-1	0	1	16980.2±7.061

***Average of three determinations ±SD**

Table 5.3 Independent and dependent variables with their levels in Box-Behnken Design

Levels			
Independent variables (Factors)	**Low (-1)**	**Medium (0)**	**High (1)**
A = Column Temperature (°C)	30	40	50
B = Flow Rate (mL/min)	0.5	1	1.5
C = Organic Phase (%)	20	50	80

Statistical analysis results	**F-Value**	***p*-Value***	**R-Sq**	**Lack of fit**
T. Plate (Y)	30.22	<0.0001	0.9749	0.5869

***p*-value < 0.05 consider as statistically significant; F-value, Fisher mean value; R-Sq, Regression Square**

5.1.2.2 Influence of independent variables on theoretical plate

The statistical analysis of quadratic model having a *p*-value of <0.0001 suggest that model is significant and best fitted for the number of the theoretical plate. Both R-square and lack of fit values 0.9749 and 0.5869 respectively indicated a good, satisfactory fit between predicted and experimental values (Table 5.3). A suitable model was selected based on *p*-value, r-square and lack of fit. After statistical evaluation and employing ANOVA, the final mathematical equation of interactions was generated by BBD:

T. Plate (Y) = +16891.10+190.64*A+137.55*B-90.04*C-48.88*AB+8.30*AC-3.52*BC+194.07*A^2+175.50*B^2+164.88*C^2

5.1.2.3 Contour and 3-D response surface methodology

Contour and 3-D response surface plot were generated to quantify the interaction between independent variables and measured response. The increase in the number of the theoretical plate was observed with increasing value of column temperature and flow rate. Significant reduction in the number of theoretical plates was noticed with raised organic phase percentage, resulting from increasing the viscosity of aqueous phase (Figure 5.2).

5.1.2.4 Chromatographic system for optimized batch

The initial chromatographic method was further optimized, and a new experimentation was made based on the optimized solution of predicted values

(Figure 5.3). The chromatographic column used was C18 4.6×150 mm with 5 µm particles.

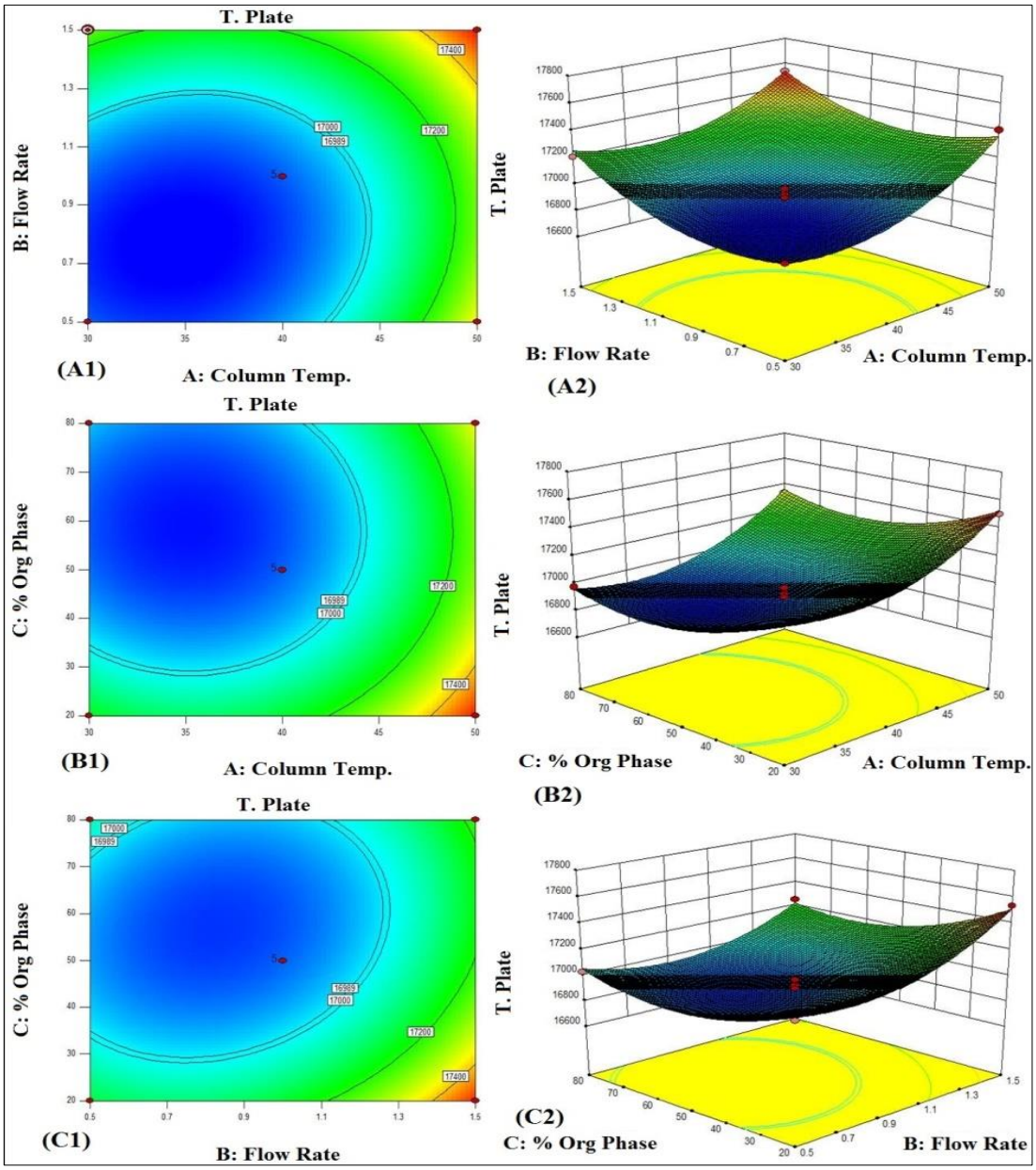

Figure 5.2 Graphical illustrations are representing the effect of independent variables (column temp., flow rate and % organic phase) on the number of theoretical plates. (A1 & A2) represents interaction effect of column temp. and flow rate on theoretical plate; (B1 & B2) describes interaction effect of column temp and % organic phase on theoretical plate; whereas (C1 & C2) represents interaction effect of flow rate and % organic phase on the theoretical plate

The mobile phase, flow rate, and column temperature were adjusted as per numerically optimized condition (Table 5.4). A quantity of 10 µL of each dilution (5, 10, 25, 50 and 100 µg/mL) was injected into the column using a flow rate of 1.49 mL/min. Each dilution was injected three times into the column, and the resultant chromatograms were obtained. The retention time was found to be 6.91 min under optimized condition.

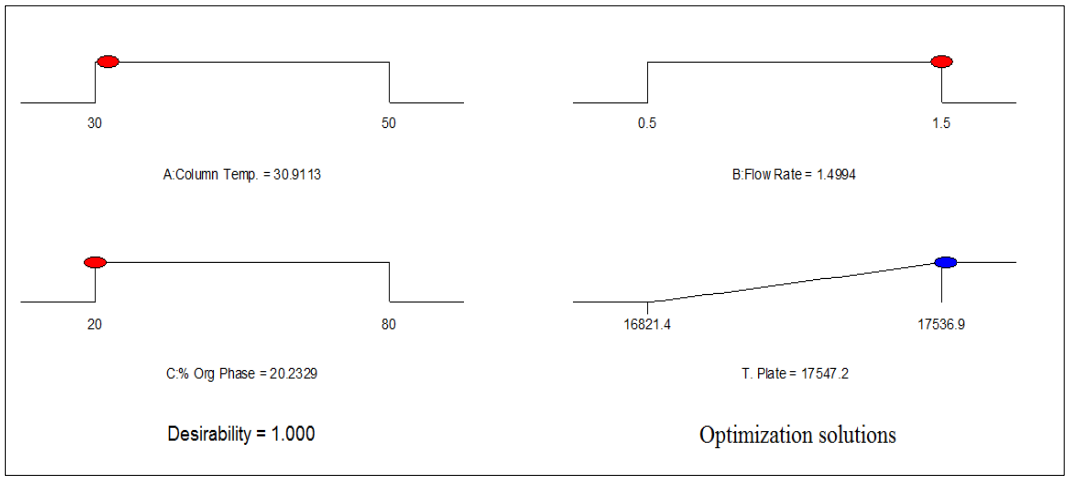

Figure 5.3 Optimized predicted values for factors as per Design Expert 10

Table 5.4 Optimization solution with predicted and experimental values

Independent variables (Factors)		
A = Column Temperature (°C)	30.91	
B = Flow Rate (mL/min)	1.49	
C = Organic Phase (%)	20.23	
Optimized results		
Dependent variable (Response)	Predicted value	Experimental value*
Y = No. of Theoretical Plates	17547.2	16883.5±8.75
Desirability	1.000	
Retention time	6.912 min	
HETP (L/N)	0.008884 µm	

***Average of three determinations ±SD**

Chromatograms of the sample at different ppm are shown in (Figure 5.4) demonstrated no interfering peaks. Drug peak symmetry was good and well resolved with minimum band spreading. The robustness study was done by creating minute changes in the chromatographic conditions at five different levels. The results of ruggedness study proved the reliability of test procedures for small changes in chromatographic conditions (Table 5.5).

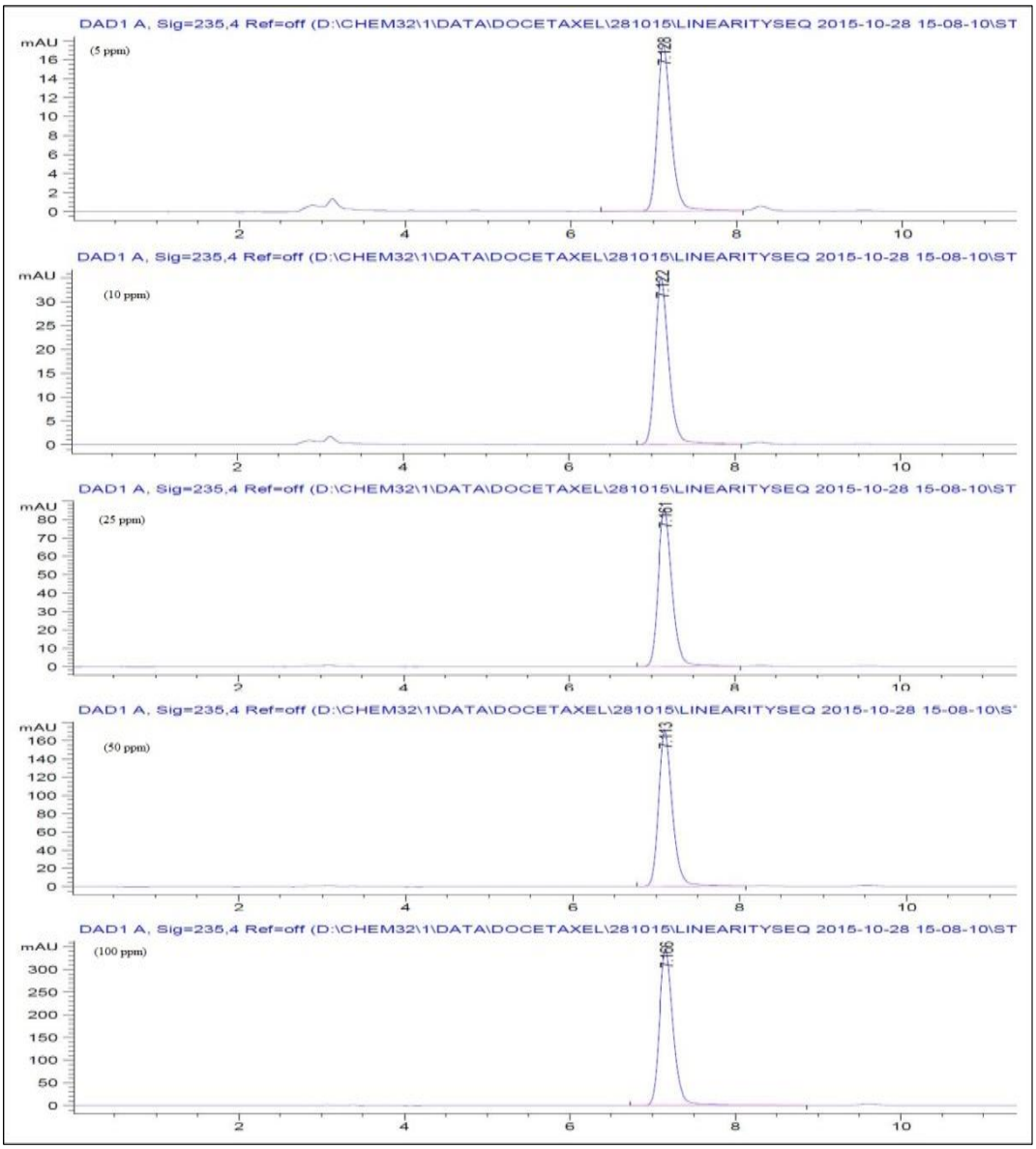

Figure 5.4 Chromatogram of docetaxel at 5, 10, 25, 50 and 100 ppm

Table 5.5 Results of ruggedness and robustness of the process

Analyst 1*		Analyst 2*		Robustness	
Samples	Area (mV)	Samples	Area (mV)	Condition and variation	%RSD
1	4332.27	1	3963.74	Solvent system (Mobile phase)	1.713
2	4271.13	2	4013.21	Wavelength (227-235)	1.129
3	4287.91	3	4173.74	Flow rate (0.5-1.5 mL/min)	1.209
4	4172.60	4	4026.71	Column temperature (30-50°C)	1.423
5	4293.16	5	4153.28	Buffer (pH 7.4 ± 0.2)	1.203
Mean	4271.414		4066.128		
SD	32.085		21.042		
RSD	1.927		1.783		

***Average of three determinations ±SD**

5.1.2.5 Analytical validation

The analytical method was validated in agreement with ICH guidelines, for precision, linearity, range, limit of detection and limit of quantification.

5.1.2.5.1 Precision

The precision of analytical method referred as the degree of closeness of the test result associated with true value and was studied to find out the intra-day and the inter-day variation in calibration curves of the drug. Both intraday (repeatability) and inter-day precision were determined by analyzing the standard solutions of its triplicate in a day and three different days. The calibration curves were generated, and percentage relative standard deviation (%RSD) was calculated. In case of reproducibility, it was performed in two separate labs and results are shown in (Table 5.6). Therefore, the precision of the method of the stressed sample was found satisfactory, reproducible and within the acceptance limit.

Table 5.6 Results of intraday, inter-day precision and reproducibility of the process

Conc.	Repeatability*		Inter-day precision*		Laboratory 1*		Laboratory 2*	
µg/mL	Conc. found±SD	%RSD	Conc. found±SD	%RSD	Conc. found±SD	%RSD	Conc. found±SD	%RSD
10	9.98±12.213	1.697	9.991±21.682	1.304	9.621±19.52	1.912	9.861±20.824	1.834
25	24.965±9.142	1.602	24.973±13.263	1.629	24.82±16.341	1.823	24.728±16.781	1.291
50	49.842±14.24	1.529	49.894±18.821	1.028	49.239±13.201	1.721	49.637±14.903	1.715

***Average of three determinations ±SD**

Concentration (µg/ml)	Linearity Results Peak area (mV)*	± SD	% RSD
0	0	0	0
5	222.78	0.0018	0.4876
10	439.62	0.0025	0.2500
25	990.45	0.0020	0.6849
50	2151.68	0.0010	0.2564
100	4332.27	0.0043	0.9033
Regression coefficient		0.9999	
Regration equation		Y=43.33x – 15.96	

*Average of three determinations.

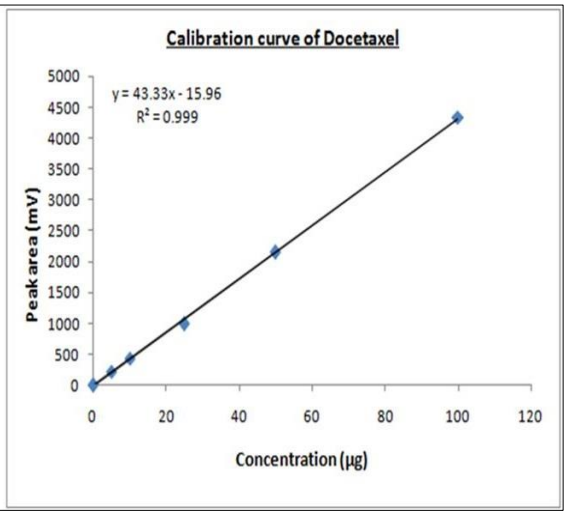

Figure 5.5 Results of linearity data and the calibration curve of Docetaxel in acetonitrile and PBS pH 7.4 (30:70) at 235 nm

5.1.2.5.2 Linearity study

From the standard stock solution, series of dilutions were made to get concentration range of 5, 10, 25, 50 and 100 µg/mL with the help of explicit solvent. HPLC was used for plotting a calibration curve of docetaxel in the concentration range of 5-100 µg/mL at 235 nm and a slope, and regression coefficient were obtained. For the

preparation of calibration curve of docetaxel, acetonitrile, and pH 7.4 saline phosphate buffer were used. The calibration curve showed in (Figure 5.5) concluding the linear relationship between peak area and the obtained concentration range within 5-100 µg/mL. The correlation coefficient of the calibration curve was found to be 0.999.

The limit of detection (LOD) and limit of quantitation (LOQ) for the drug were calculated based on standard deviation of y- intercept of the regression line and the slope of the calibration curve at levels approximating the LOD and LOQ. LOD and LOQ value of optimized method were found to be 0.042 µg/mL and 0.15 µg/mL respectively with signal to noise ratio of 3.3 and 10 for assay validation as per ICH Q2 (R1) guidelines (Table 5.7).

Table 5.7 Results of the limit of detection and limit of quantitation

LOD		**LOQ**	
Conc. (µg/mL)	S/N ratio	Conc. (µg/mL)	S/N ratio
0.042	3.3	0.15	10

5.1.2.5.3 Stability indicating degradation studies

Docetaxel was subjected to various degradation conditions like acidic, alkaline, oxidation, thermal, photodegradation and neutral conditions for 72 h. The drug was found to be highly degraded at oxidation and comparatively stable under neutral condition (Figure 5.6).

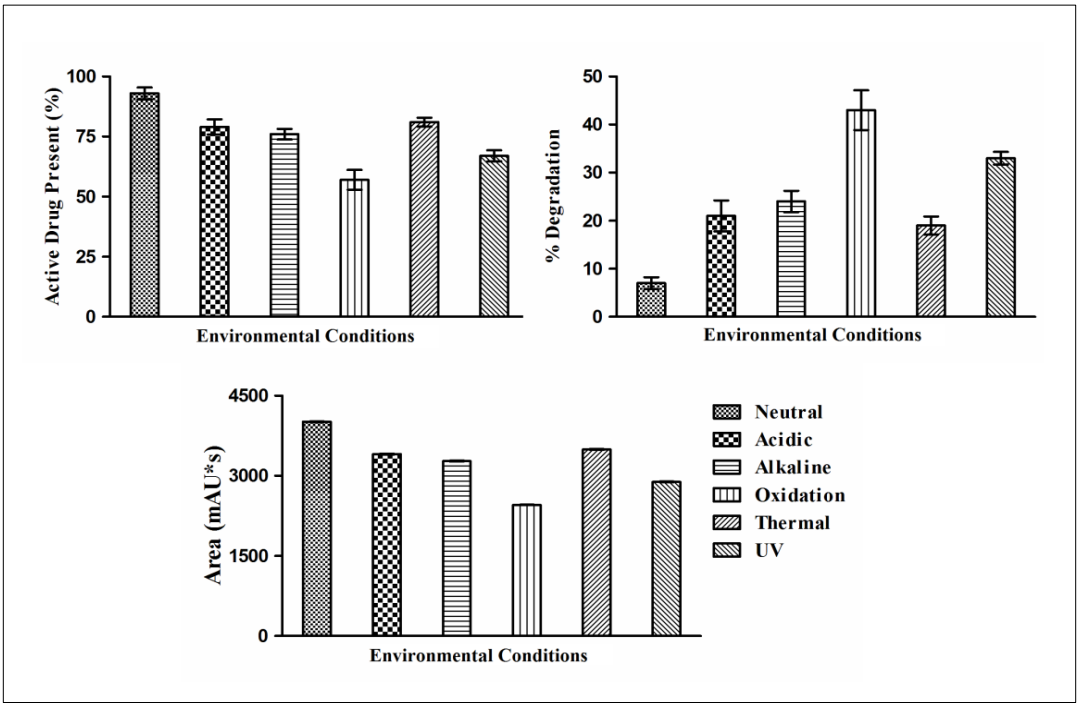

Figure 5.6 Degradation data for docetaxel at various environmental conditions for 72 h (vertical bars represent average of three determinations ±SD)

5.1.3 Conclusion

The HPLC method development utilizing quality by design was successfully passed through validation which provides an assurance of quality for the method. A multidimensional approach formed by independent variables using Box-Behnken Design which allowed a limited amount of data to examine large numbers of possible run condition to demonstrate the robustness of the process. These designs of experiment with software approaches enable us to gain insight of the multifactorial variability of high-performance chromatography. The stability-indicating HPLC method was developed and validated. The developed method was found to be precise, accurate and sensitive.

5.2 Preparation of PHBV-PVA-DTX polymeric nanoparticles

5.2.1 Plackett-Burman Design

PBD helps in limiting the number of experiments over a large number of variables. A total of twelve experimental runs were generated from ten factors, four responses, and two levels PBD statistical experiment. The independent variables, responses, and design matrix are given in Table 5.8. The statistical evaluation of result was conducted by applying ANOVA, and finally, Pareto charts were generated to screen out the most significant independent variables influencing response (Figure 5.7).

Table 5.8 Plackett-Burman Design matrix representing experimental runs with independent variables and their observed responses

Run	PHBV	PVA	SOLVENT	H. SPEED	H. TIME	US TIME	S. SPEED	S. TIME	C. SPEED	C. TIME	P. SIZE (nm)	ZP (mV)	PDI	%EE
1	-1	-1	1	1	1	-1	1	1	-1	1	255	-14	0.29	37
2	-1	-1	-1	-1	-1	-1	-1	-1	-1	-1	253	-14	0.29	28
3	-1	1	1	1	-1	1	1	-1	1	-1	247	-19	0.16	34
4	-1	-1	-1	1	1	1	-1	1	1	-1	245	-16	0.31	35
5	1	-1	1	-1	-1	-1	1	1	1	-1	274	-15	0.27	38
6	1	1	1	-1	1	1	-1	1	-1	-1	256	-18	0.15	39
7	1	-1	1	1	-1	1	-1	-1	-1	1	271	-14	0.26	41
8	-1	1	1	-1	1	-1	-1	-1	1	1	246	-17	0.15	30
9	1	1	-1	1	-1	-1	-1	1	1	1	277	-20	0.16	40
10	-1	1	-1	-1	-1	1	1	1	-1	1	244	-19	0.17	32
11	1	-1	-1	-1	1	1	1	-1	1	1	262	-13	0.28	41
12	1	1	-1	1	1	-1	1	-1	-1	-1	274	-18	0.13	44

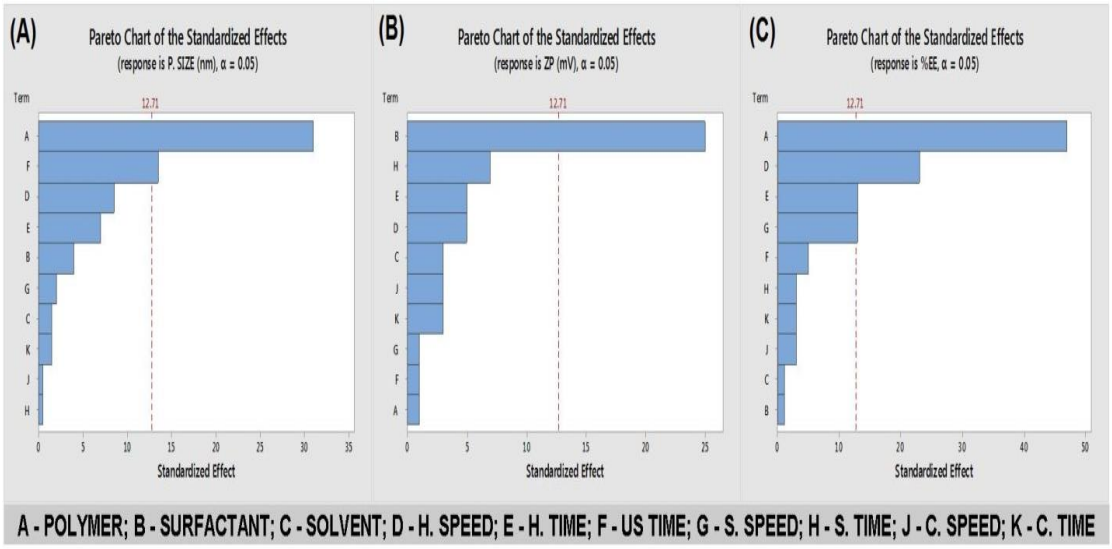

Figure 5.7 Pareto chart showing the influence of variables on responses; (A) influence of input variables on particle size, (B) influence of input variables on zeta potential, (C) influence of input variables on entrapment efficiency

5.2.2 Box-Behnken Design

Box- Behnken experimental design was employed consisting of 3 levels, 5 factors and 6 center points (Table 5.9). Design matrix of BBD comprises of 46 runs recognized by Design-Expert 10 software. An analysis of variance (ANOVA) was performed at 95% confidence interval to test the significance of all coefficients and eliminate the less significant factors. The quadratic equations were generated for each response which is denoted by positive and negative sign corresponding to their synergistic and antagonistic effect respectively. The effects on particle size, zeta potential, and entrapment efficiency are shown (Table 5.10) in the form of coded factors determined by Design expert 10. Contour and 3-D response surface plot were generated to quantify the correlation and interaction between independent variables and measured response (Figure 5.8). Statistical analysis of quadratic model summary

(Table 5.11) revealed significant *p*-value and lack of fit for all responses [Beg et al., 2013, Cao et al., 2013].

Table 5.9 Independent and dependent variables with their levels in Box-Behnken design

Levels			
Independent variables (Factors)	**Low (-1)**	**Medium (0)**	**High (1)**
A. Polymer (%w/v)	3%	11.5%	20%
B. Surfactant (%w/v)	1%	2.5%	4%
C. Homogenizer Speed (rpm)	10,000	15,000	20,000
D. Homogenization Time (min)	5 min	7.5 min	10 min
E. Ultra Sonication Time (min)	5 min	7.5 min	10 min

Dependent variable (Response)	**Constraint**
Y_1 = Particle size	200-350
Y_2 = Zeta potential (mV)	Minimize
Y_3 = Entrapment efficiency (%)	Maximize

Table 5.10 Quadratic equation generated by BBD

Y	**P. Size**	**Zeta P.**	**EE**
X_0	+352.83	-15.83	+36.50
*** A**	+103.31	+2.386E-015	+7.62
*** B**	-2.75	-5.12	-0.38
*** C**	-2.37	-0.062	-0.38
*** D**	+10.88	-0.44	+0.063
*** E**	-55.94	+1.806E-034	-0.063
*** AB**	+5.00	-0.25	+0.25
*** AC**	+9.25	-1.00	-0.50
*** AD**	-0.50	-0.25	+0.50
*** AE**	+13.50	-0.50	+0.75
*** BC**	-12.00	+3.238E-017	+0.50
*** BD**	+1.75	+0.25	-1.75
*** BE**	-1.25	+7.951E-017	+1.00
*** CD**	+2.705E-015	-1.25	+5.806E-017
*** CE**	+0.75	+0.50	-1.00
*** DE**	-1.75	+0.50	-1.50

* A^2	+5.60	+0.29	-1.60
* B^2	+2.52	-0.042	+0.73
* C^2	+5.52	-0.12	+0.73
* D^2	+2.69	+0.042	+0.98
* E^2	-41.23	+0.29	+0.48

***Y= response; X_0 = intercept; A-E= factors; ** positive value of independent factor represents direct and negative value represents indirect effect on response**

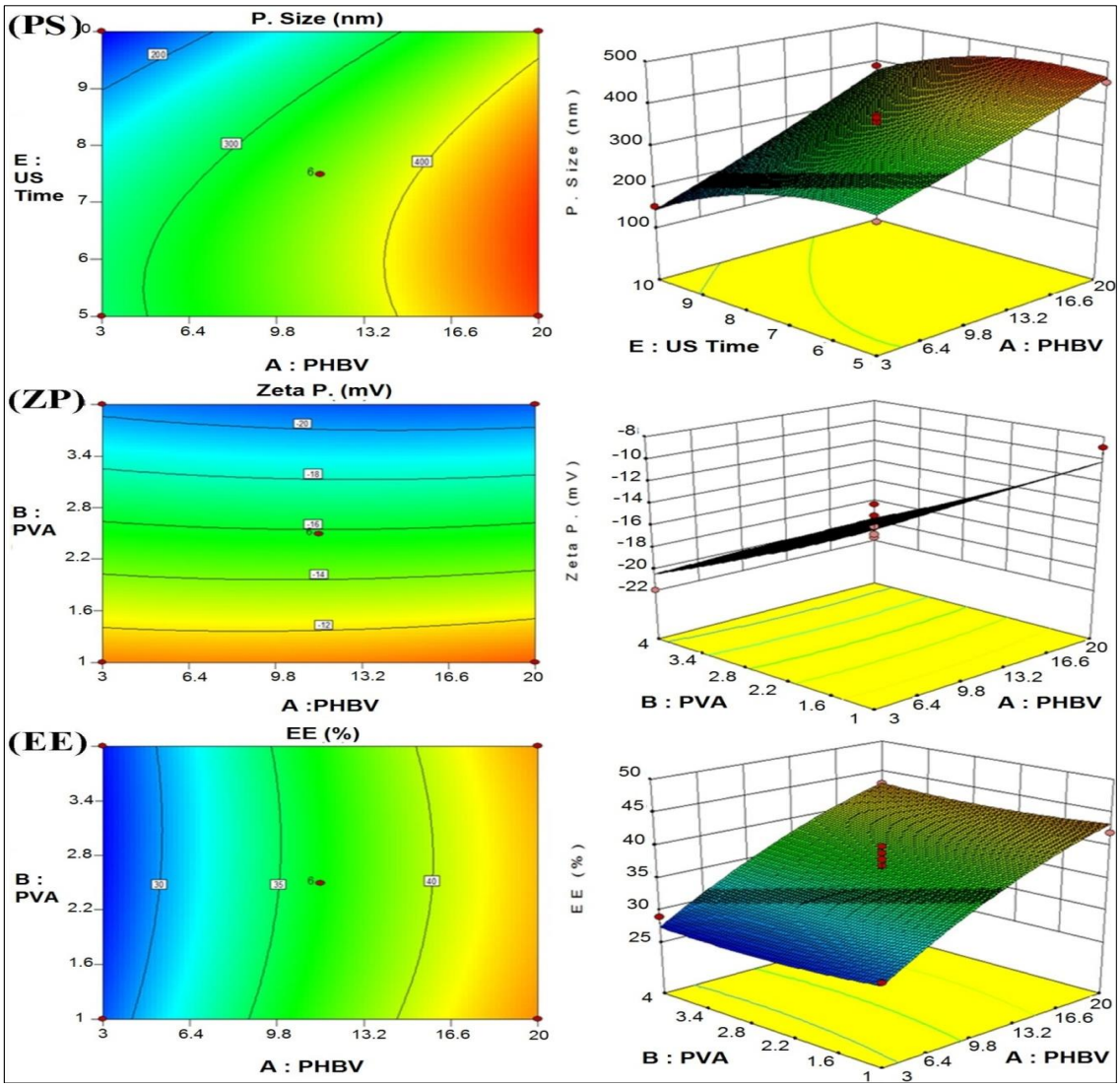

Figure 5.8 Contour and 3-D Response Surface Methodology showing effect of independent variables on responses; (PS) effect of input variables on particle size, (ZP) effect of input variables on zeta potential and (EE) effect of input variables on % entrapment efficiency

Optimization and validation of batch were performed by numerical optimization technique where predicted values were found via optimization plot by fixing the constraints for all independent variables. Furthermore, a new batch of NPs with predicted values of independent variables was prepared (Table 5.12). As predicted values showed reasonable good agreement and a low percentage of bias with experimental results, it confirms the validity of optimization. Thus, the results obtained reaffirmed the reliability of an optimized batch and were selected for further studies.

Table 5.11 Statistical ANOVA analysis results of quadratic model

Response	**Quadratic model**							
	F-Value	*p*-Value*	R-Sq	R-Sq (adj)	R-Sq (pred)	CV %	Lack of fit	Remark
P. Size	34.40	0.0001	0.9649	0.9369	0.8739	5.48	0.4046	Significant
ZP (mV)	15.78	0.0001	0.9266	0.8679	0.7434	7.53	0.5447	Significant
%EE	10.24	0.0001	0.8912	0.8042	0.7107	6.05	0.9927	Significant

***p*-value < 0.05 consider as statistically significant; F-value, fisher mean value; *P*-value, probability value; R-Sq, regression square ; R-Sq(adj), adjusted R-Sq; R-Sq(pred), predicted R-Sq ; CV%, coefficient of variation.**

Table 5.12 Results of optimization utilizing Box-Behnken design

Independent variables for response optimization	
A = PHBV	15.29 mg
B = PVA	3.96 mg
C = H. Speed	10,718 rpm
D = H. Time	5 min
E = US Time	10 min

Optimized results		
Dependent variable (Response)	Predicted value	Experimental value*
Y_1 = Particle size	318	283±2.79
Y_2 = Zeta potential (mV)	-22.10	-17.52±2.64
Y_3= Entrapment efficiency (%)	46	44±0.59

***Average of three determinations ±SD**

5.2.2.1 Influence of independent variables on particle size

The particle size of NPs was varied in the range from 200 nm to 350 nm as a consequence of the change in formulation variables. The mathematical polynomial equation generated by multiple linear regressions with constant and regression coefficients for particle size is given in Table 5.10. The quadratic model having F-value of 34.40 and *p*-value of <0.0001 suggests that it is the best fitted for particle size. The value of regression coefficient was found to be 0.9649, indicating a good fit between predicted values and experimental values. The lack of fit *p*-value of the model was 0.4046 implies that the quadratic model had no lack of fit ($p>0.05$). Therefore, this model can be used to plot the design space and response optimizer. The concentration of PHBV polymer seems to be one of the most leading parameters influencing the particle size directly. Polymeric concentration with high value enhances the viscosity of organic phase, which decreases the stirring efficiency. Hence, resists the progress of emulsion droplet to break, resulting in a larger particle. Ultrasonication time holds an inverse relation with particle size, with increase in the shear stress leading to the formation of the smaller sized particle. Surfactant concentration and homogenization speed also imparts negative correlation and protects particles to grow into bigger ones.

5.2.2.2 Influence of independent variables on zeta potential

The NPs possessed zeta potential in the range of -13 to -20 for certain levels of variables suggesting homogeneous distribution with long term stability. The mathematical polynomial equation explaining the effect of the independent variables on zeta potential was obtained by regression given in Table 5.10. The F-value of the

quadratic model was 15.78 with a very low *p*-value of <0.0001. The regression coefficient of the model was found to be 0.9266, indicating a good fit. The model showed adequate fitting to data as lack of fit was absent due to having a *p*-value of 0.5447 (p>0.05). Whereas evaluating zeta potential as a response, the significant increment was observed with a consequent increase in surfactant concentration which might be due to the reduction of interfacial tension.

5.2.2.3 Influence of independent variables on entrapment efficiency

The entrapment efficiency of NPs varied in the range of 30% to 44% for various factors level combinations in the formulations. The effect of the independent variables on drug entrapment efficiency can be explained by the mathematical polynomial equation mentioned in Table 5.10. The quadratic model was found to be significant with F-value of 10.24 (p<0.0001). The value of regression coefficient was found to be 0.8912, indicating a good adequacy and fit of the model. The model implies adequate fitting to data showing a *p*-value of 0.9927 (p>0.05) as the lack of fit. The enhanced entrapment efficiency with a relative increase in PHBV polymer concentration was observed on account of more availability of polymer for encapsulating the drug. Surfactant concentration would have no such significant effect on entrapment efficiency.

5.2.3 Morphological study

AFM micrographs are three-dimensional images used to observe the external surface morphology of drug loaded NPs. Here, the nanoformulation was diluted, and a drop of it was placed on a small microscopical slide to obtain a thin, dry film. It was

further visualized by scanning probe microscope NT-MDT (Figure 5.9c) by mounting on the scanner. Atomic force microscopy (AFM) images showed uniform spherical shaped NPs having a smooth surface without having any visible pores and agglomerates, indicated that PVA stabilized them. Transmission electron microscopy (TEM) studies are performed to establish a direct comparison of individual particle size of sonicated nanoparticles. A drop of sample was placed onto a carbon-coated copper grid to leave a thin film, and excess of solution was drained off by using filter paper. The grid was allowed to air dry thoroughly, and samples were viewed using transmission electron microscope (TECHNAI-20G^2, Czech Republic). HR-TEM of the drug loaded optimized NPs formulation showed discrete, homogeneous and spherical particles within the size range of 200-300 nm (Figure 5.9a). Also, the surface morphology of optimized NPs was visualized by Scanning electron microscopy (SEM, Carl Zeiss Inc., USA) under 10K X magnifications and was found to be of spherical shape and smooth surface (Figure 5.9b).

5.2.4 Average particle size and zeta potential

Average particle size and size distribution of the nanoparticle was measured using particle size analyzer (Desla Nano C, Beckman Coulter, USA) instrument at 25°C where brownian motion and light scattering determines the diameter of NPs. The zeta potential of the colloidal system mainly depends on the chemical nature of the polymer, surfactant, and drug used. Zeta potential of optimized NP formulation was found to be -17.52 mV which justifies the stability of the colloidal system (Table 5.12), as the negative charge will reduce protein binding and thus, is less likely to activate immune system resulting in longer circulatory life.

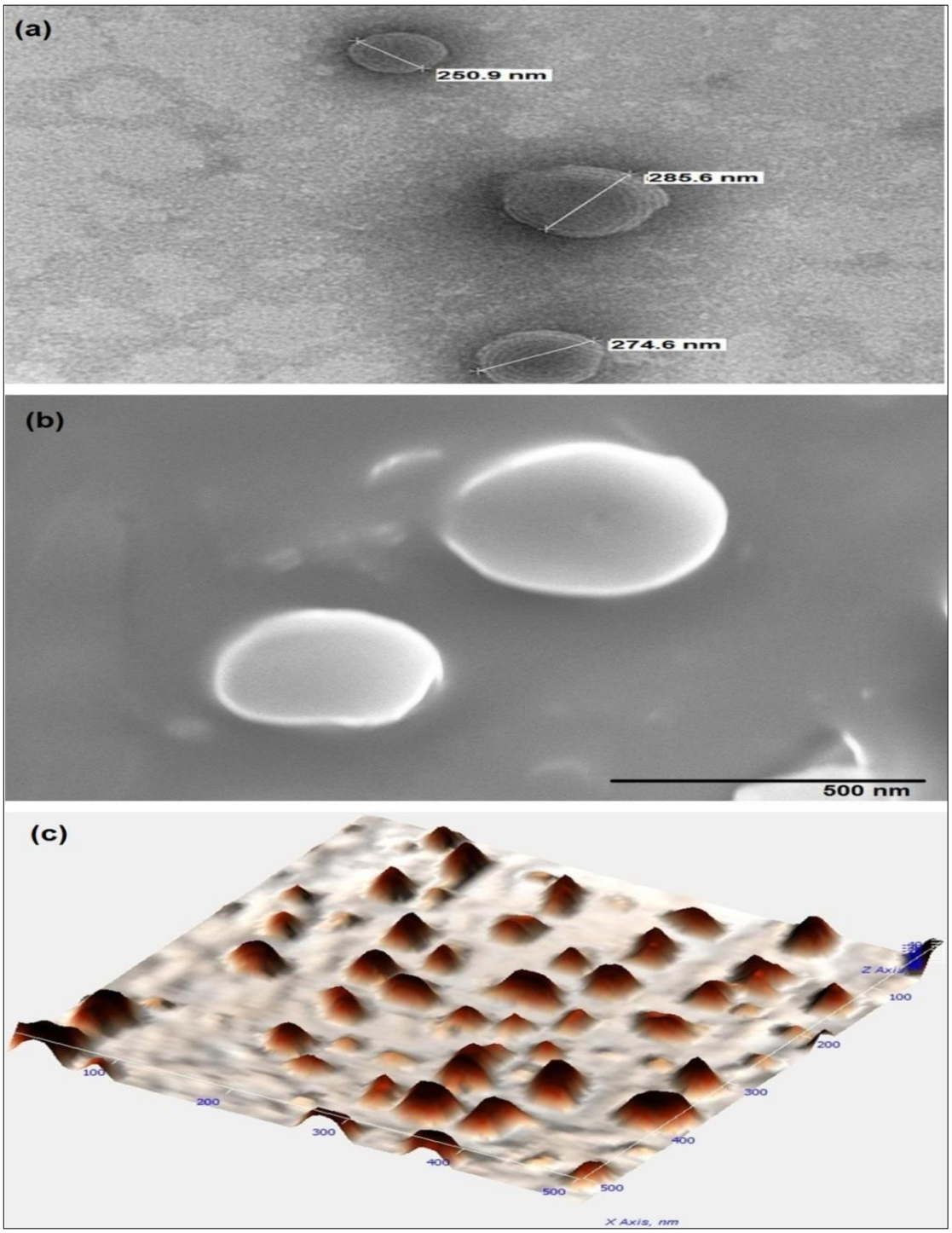

Figure 5.9 (a) HR-TEM image; (b) SEM image at 10KX of optimized formulation and (c) AFM micrograph

5.2.5 In vitro release of docetaxel

The retention of potent antineoplastic drugs within the NPs is crucial for the clinical application. In Figure 5.10, the release data of docetaxel from PHBV NPs in PBS pH 7.4 at 25°C demonstrates minimal drug release for 3-4 days period. This less liberation of drug provides a window of toxicity protection during circulation and allowing specificity to leaky blood vasculature of tumors by EPR effect. The release data were then fitted to various empirical equations to evaluate the regression coefficients. The highest regression coefficient of 0.918 was observed for the Peppas-Korsmeyer model, indicating polymer disentanglement and erosion dominated the drug release rate.

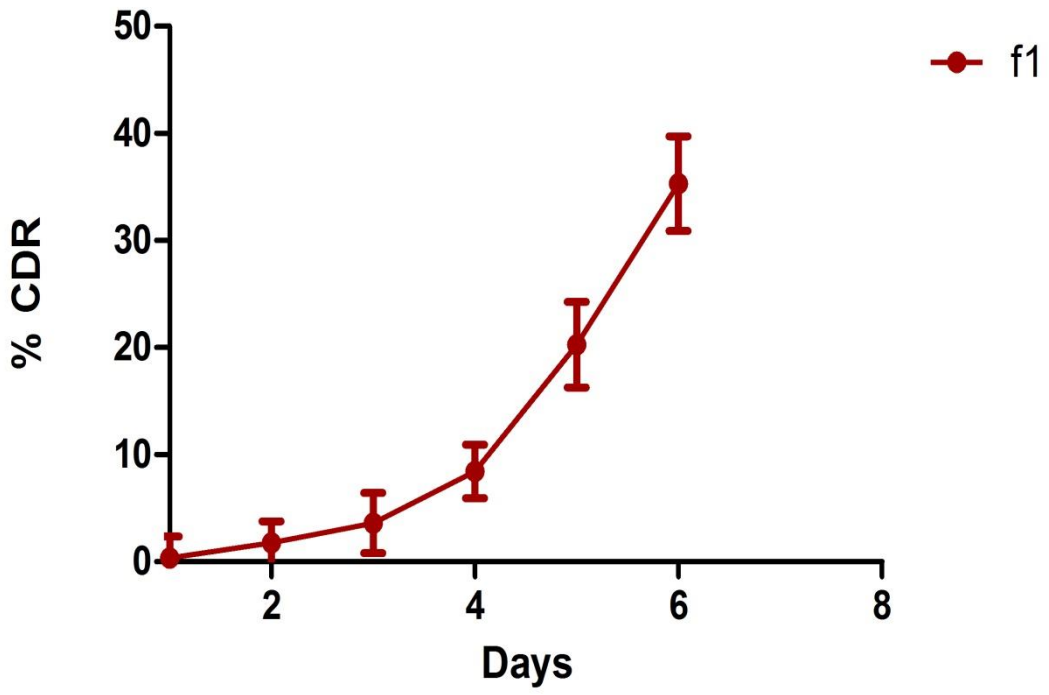

Figure 5.10 *In vitro* percentage cumulative release profile of drug from NP in PBS pH 7.4 (vertical bars represent average of three determinations ±SD)

5.3 Preparation of PHBV-PF127-DTX polymeric nanoparticles

5.3.1 Plackett-Burman screening studies

During the formulation process of PHBV nanoparticles, numbers of parameters such as polymer concentration, concentration of surfactant, water/organic phase ratio, homogenization speed/time, sonication time, stirring speed/time and centrifugation speed/time were involved and helpful in optimization process in order to improve particle size, zeta potential, PDI and percentage entrapment efficiency. The selection of parameters was mainly done by identifying CMA (critical material attributes) and CPP (critical process parameter). Further, this information was used to find their critical quality attributes by utilizing failure mode effect analysis following literature survey. In respect to screen these various parameters over a fewer run, we have selected Plackett-Burman Design (PBD). Here, we used Pareto chart and half normal plot to screen out the numbers of factors by using Minitab 17 software (Figure 5.11). Twelve experimental runs were generated from ten independent variables and four responses by applying two levels of statistical experiments. These screened factors were further used in Box-Behnken design (BBD) for response surface methodology (RSM) studies of formulation optimization.

5.3.2 Optimization and statistical analysis

In this study, 5-independent variables, 3-responses and 46-experimental run were implicated and analyzed using Design Expert 10 software. Based on statistical parameters, the effects and interaction of independent variables which include polymer concentration, surfactant concentration, homogenizer speed, homogenization time and ultrasonication time, over responses were determined

(Table 5.13). The optimum values of variables were determined based on ANOVA, polynomial equations, correlation coefficient, adjusted multiple correlation and sum of squares (Table 5.13).

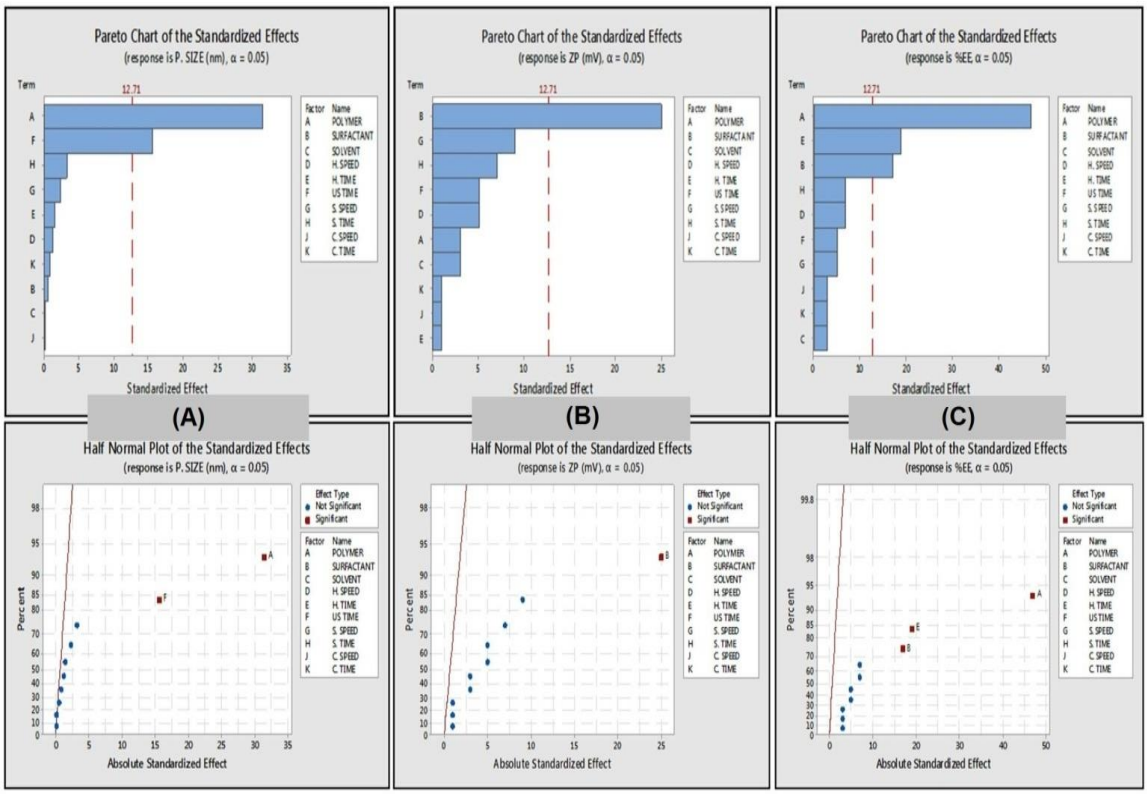

Figure 5.11 Pareto chart and half normal plot showing the influence of variables on responses; (A) influence of input variables on particle size, (B) influence of input variables on zeta potential, (C) influence of input variables on entrapment efficiency

Response surface plots in contour and three-dimensional plots were used to identify the relationship between factors and responses (Figure 5.12). In the quadratic equation, the positive value indicates constructive effect, while the negative value suggests an antagonistic effect on independent variables and measured responses (Table 5.14). By numerical optimization technique, predicted values were generated for all the responses, which showed good agreement with experimental results and

the low percentage of bias, suggesting the reliability and reasonability of optimization process. The highest % entrapment efficiency with required particle size and zeta potential was achieved by using optimal conditions of 18.38 mg PHBV, 4 mg PF-127, 10,000 rpm homogenizer speed, 5 min homogenization time and 9.40 min ultrasonication time with desirability one (Table 5.13).

Table 5.13 Independent and dependent variables with their levels in Box-Behnken design

Levels **Independent variables (Factors)**	**Low (-1)**	**Medium (0)**	**High (1)**	**BBD Results**
A.Polymer (%w/v)	3	11.5	20	18.38 mg
B.Surfactant (%w/v)	1	2.5	4	4 mg
C.Homogenizer Speed (rpm)	10,000	15,000	20,000	10,000
D.Homogenization Time (min)	5	7.5	10	5
E.Ultra Sonication Time (min)	5	7.5	10	9.40

Dependent variable (Response)	**Constraint**	**Predicted value**	**Experimental value****
Y_1= Particle size (nm)	200-350	338.5	260±2.85
Y_2= Zeta potential (mV)	Minimize	-21.09	-18±2.12
Y_3= Entrapment efficiency (%)	Maximize	47.13	39±0.85

Statistical ANOVA analysis of Quadratic model					
	F-Value	***p*-Value***	**R-Square**	**Lack of fit**	**Remarks**
Particle Size	43.40	0.0001	0.9720	0.5724	Significant
Zeta Potential	12.20	0.0001	0.9071	0.8037	Significant
% E. Efficiency	22.54	0.0001	0.9475	0.9020	Significant

***p*-value < 0.05 consider as statistically significant;**Average of three determinations ±SD**

5.3.2.1 Influence of independent variables on particle size

The particle size of optimized nanoparticle was in the range from 493 nm to 237 nm as per the effect of the change in formulation variables. The mathematical equation generated by polynomial regressions model for particle size is given in Table 5.14.

The quadratic model having F-value of 43.40 and *p*-value of <0.0001 suggests the best fit. The value of regression coefficient (R^2-0.9720) was indicating a good fit between predicted values and experimental values. The lack of fit value of the model was found to be 0.5724 implies no lack of fit (p>0.05) model. Therefore, this quadratic model can significantly be used to plot the optimized design space. The PHBV concentration seems to be one of the most selected variables influencing the particle size strongly. PHBV concentration with high value enhances the viscosity of organic phase, which resists the development of emulsion droplet to break, resulting in a larger particle. Ultrasonication time holds an inverse relationship with particle size, with increase in the time of sonication the particle size of the formulations were decreased. The concentration of PF-127 and the speed of homogenization impart a negative correlation and due to this decrease in particle size seen.

5.3.2.2 Influence of independent variables on zeta potential

The prepared NPs possessed zeta potential in the range of -9 to -22, suggesting homogeneous distribution of formulation with long-term stability. The mathematical quadratic response explaining the effect of the independent variables on zeta potential is given in Table 5.14. The F-value of the quadratic model was 12.20 with a slight *p*-value of <0.0001. The regression coefficient of the model was found to be 0.9071, indicating a good fit. The model showed sufficient satisfactory data as lack of fit having a *p*-value of 0.8037 (p>0.05). Whereas evaluating zeta potential as a response, the significant percentage increase was observed with increase in PF 127 surfactant concentration due to reduction of interfacial tension.

Table 5.14 Quadratic equation generated by BBD

Y	P. Size	Zeta P.	EE
X_0	+369.67	-16.83	+36.50
*** A**	+103.50	+0.31	+7.62
*** B**	-2.69	-5.06	-0.19
*** C**	+2.37	+0.25	-0.13
*** D**	-0.19	-0.44	-0.44
*** E**	-40.75	+0.19	-0.25
*** AB**	-1.00	+0.50	-0.50
*** AC**	+17.75	-0.25	+0.25
*** AD**	-4.50	+0.50	-0.50
*** AE**	-3.25	-0.50	+1.75
*** BC**	+8.50	+1.00	-1.50
*** BD**	-2.75	+1.214E-017	-0.25
*** BE**	-1.50	-0.25	-2.194E-016
*** CD**	-2.75	-0.25	-1.00
*** CE**	+4.50	-0.50	-0.25
*** DE**	-1.75	-1.031E-016	+1.165E-016
*** A^2**	-4.73	+0.19	+0.71
*** B^2**	-4.15	+0.85	+1.13
*** C^2**	-9.06	+0.10	+0.21
*** D^2**	-7.65	+0.19	+1.12
*** E^2**	-51.40	+0.19	-0.79

***Y= response; X_0 = intercept; A-E= factors; ** positive value of independent factor represents direct and negative value represents indirect effect on response**

5.3.2.3 Influence of independent variables on entrapment efficiency

The entrapment efficiency of optimized formulation was found in the range of 27% to 46% for various factors level combinations in the formulation. The mathematical polynomial equation mentioned in Table 5.14, explains the effect of the independent factors on entrapment efficiency of the drug. The quadratic model of the formulation was found to be significant with F value of 22.54 ($p<0.0001$). The value of

regression coefficient (0.9475), demonstrating good adequacy and fit of the model. The model implies satisfactory fitting to data presentation a *p*-value of 0.9020 ($p>0.05$) as the lack of fit. The improved entrapment efficiency with a relative increase in the concentration of polymer was observed on an explanation of more availability of PHBV for encapsulation. Surfactant concentration would have no such significant effect on entrapment efficiency.

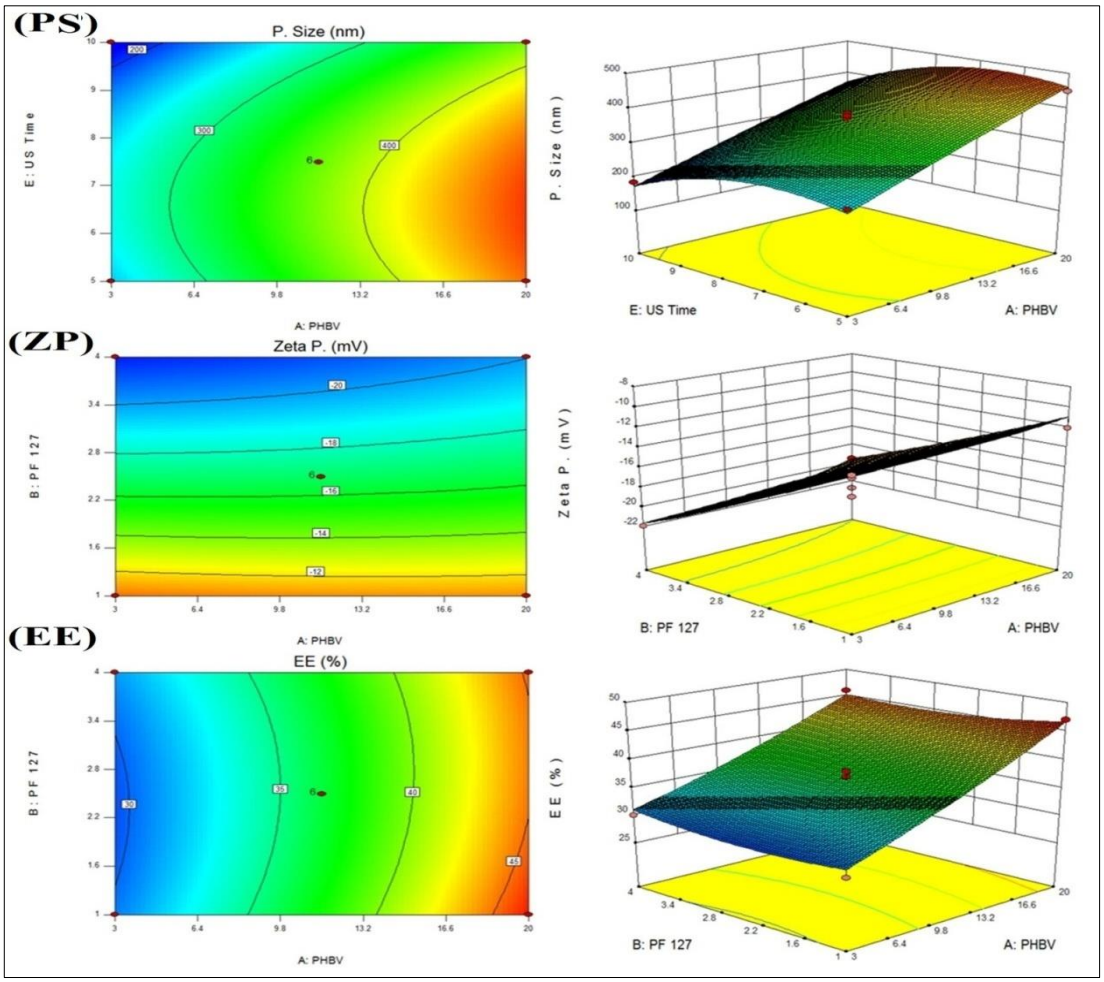

Figure 5.12 Graphical illustrations of Contour and 3-D Response Surface Methodology showing the effect of independent variables on responses; (PS) effect of input variables on particle size, (ZP) effect of input variables on zeta potential and (EE) effect of input variables on percentage entrapment efficiency

5.3.3 Morphological study

Figure 5.13, represents the micrographs of optimized PHBV NPs which were obtained by (A) SEM, (B) TEM and (C) AFM. SEM image of NPs were visualized by Carl Zeiss Inc., USA under 10 KX magnifications. TEM study was done by placing a drop of the sample in the middle of a carbon-coated copper grid which was viewed using TECHNAI-20G^2, Czech Republic. AFM micrograph is a three-dimensional image, visualized by scanning probe microscope NT-MDT, Russia by mounting a dry, thin film on the scanner. It could be seen that spherical nanoformulation was formed with no sign of agglomeration. The optimized NP formulation was found to be spherical in shape with a smooth surface and uniform size distribution.

5.3.4 Average particle size and zeta potential

The particle size of the optimized batch was obtained as 260±2.85 nm with polydispersity size distribution. Among all, the significant factor concentration of polymer predominantly influenced the size of nanoparticles. The nano size of the particulate system provides higher surface area and more availability within the blood vessels of tumor tissue to achieve better permeation and retention effect. The zeta potential analysis is the crucial parameter as it affects the physical stability and *in vivo* fate of Nanoparticles. The surface charge of optimized batch was found to be -18±2.12 mV with no significant difference between each preparation. The negative value ensures long-term stability and avoids aggregation of particles. The presence of PF-127 on nanoparticle surface formed stable colloidal suspension due to steric repulsion forces between particles. Hence, it reduces the opsonization process and

protein binding within the body and results in a longer circulatory life of Nanoparticles.

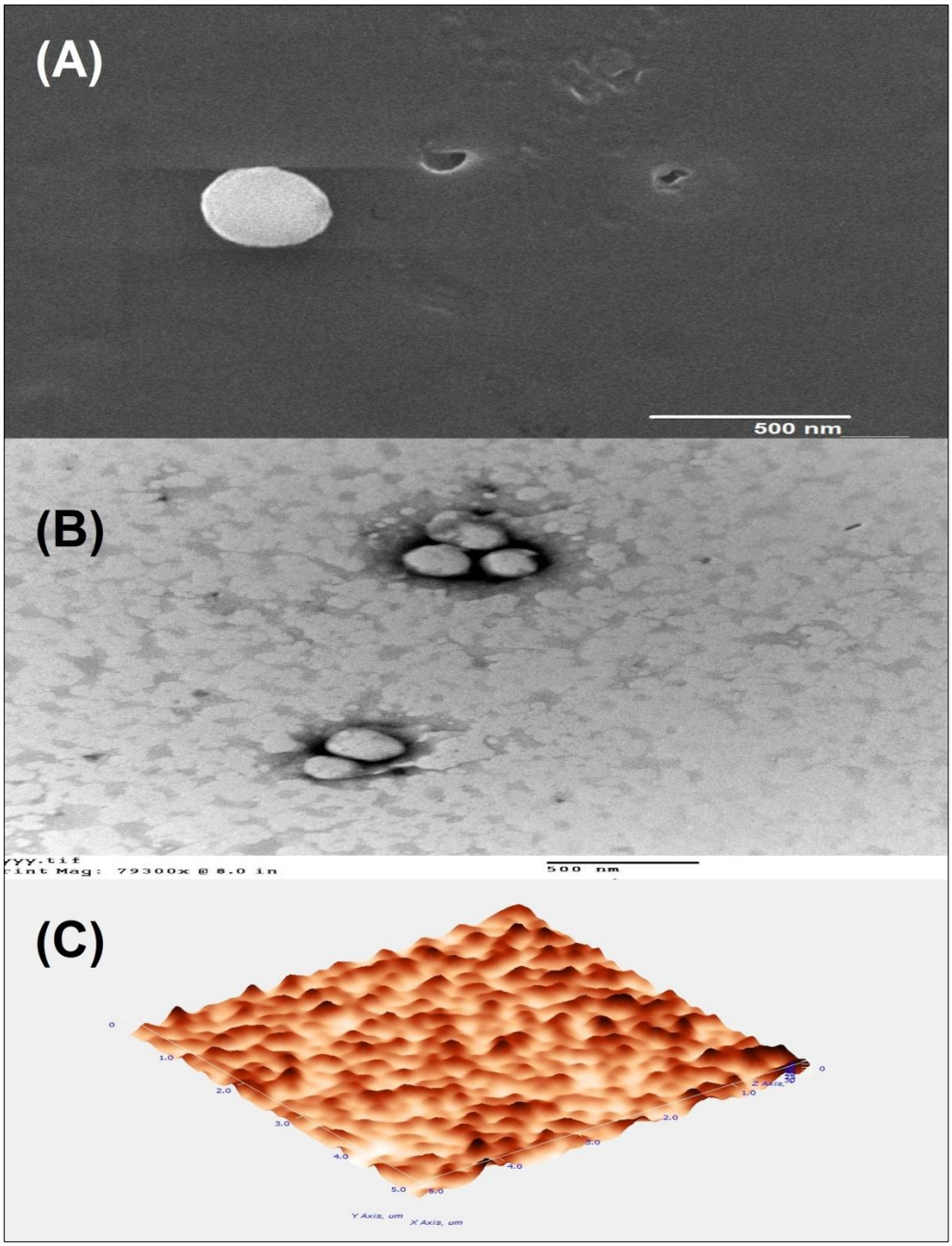

Figure 5.13 (A) SEM micrograph; (B) HR-TEM image; (C) AFM image of the optimized formulation

5.3.5 In vitro drug release

Drug release study was investigated using a dialysis membrane in a non-biological condition of phosphate buffer saline pH 7.4 at 37±0.5°C. The liberation of docetaxel from PHBV nanoparticle is shown in Figure 5.14, where docetaxel exhibited a slow release from PHBV nanoparticles indicated delayed followed by sustained release as released less than 11% drug over 48 h. The formulation showed release without burst effect may be due to lack of free drug at the surface of PHBV nanoparticles. The sustained release of drug from the PHBV nanoparticles suggests high specificity for prolonging the circulation time in *in vitro* condition to meet EPR effect. The mechanism of drug release was determined by the R^2 value for each kinetic model. Out of release data obtained from zero-order, first-order, Higuchi and Korsmeyer-Peppas, zero order model was found to be the best fit (R^2 = 0.977) having much larger R^2 value than other kinetic models. Thus, it can be said that the drug release follows zero order drug release kinetics and can provide continuous delivery of drug with controlled rate to achieve a prolonged action.

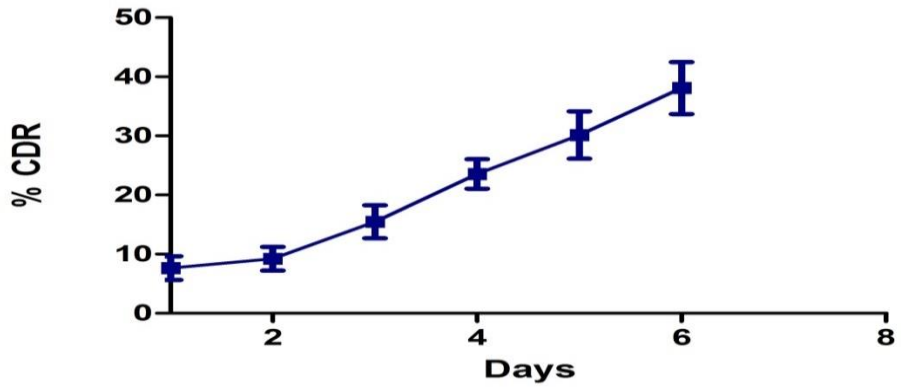

Figure 5.14 Profile showing *in vitro* cumulative percentage drug release from PHBV NPs in PBS pH 7.4 (vertical bars represent average of three determinations ±SD)

5.4 Preparation of PHBV-TPGS-DTX polymeric nanoparticles

5.4.1 Optimization studies

The identification of critical material attributes (CMA) and critical process parameter (CPP) influencing the development of optimized nano formulation is a prerequisite of quality by design (QBD). The essential critical quality attributes (CQA) were chosen as a factor by a simple method of control impact matrix (Table 5.15) and failure mode effect and critical analysis studies (FMECA) based on risk priority number (RPN) of severity, occurrence, and detection (Table 5.16). RPN above 100 was considered to be a high-risk factor in accordance to critical to quality (CTQ) which is essential for the quality product [Shahin, 2004]. FMECA identifies the estimated risk associated with specific cause and prioritizes the action taken to reduce the risk [Guideline, 2005]. The results obtained from FMECA studies were further subjected to screening design.

Table 5.15 Control Impact Matrix

CQAs	Important	Moderate	Not Important
In Control	Drug Polymer Surfactant Homogenizer Probe sonicator	Formulator Solubility Magnetic stirrer Solvent Centrifuge	----------
Out of Control	Particle Size Zeta potential Drug Entrapment Drug release	Temperature Contamination UV/FTIR/HPLC Lyophilizer	Humidity Pressure

Table 5.16 FMECA analysis based on severity, occurrence, detection, criticality and risk priority number

CTQ (Independent Variables)	**FMECA (failure mode effect & critical analysis)**				
	Severity (S)	Occurrence (O)	Detection (D)	Criticality (S*O)	**RPN** (S*O*D)
Polymer type	6	4	3	24	72
Polymer conc.	8	5	4	40	160
Surfactant type	6	4	4	24	96
Surfactant conc.	7	5	5	35	175
Solvent type	6	4	4	24	96
Solvent ratio	5	6	3	30	90
Solubility	6	5	3	30	90
Homogenizer speed	7	6	3	42	126
Homogenization time	4	5	5	20	100
Sonication time	7	6	3	42	126
Stirring speed	4	4	3	16	48
Stirring time	6	5	3	30	90
Centrifugation speed	5	5	3	25	75
Centrifugation time	4	4	2	16	32

5.4.2 Plackett-Burman factor screening design

When the number of factors is huge, the screening experiments are used to reduce the sets of factors to those that are most influential to the response. Factor screening by design was carried out by the DOE approach of 5 factors, one block, one replicate, two-level Plackett-Burman design using Minitab™ 17 software. The independent variables used in this experimentation were (A) concentration of PHBV, (B) concentration of TPGS, (C) homogenizer speed, (D) homogenization time and (E) ultrasonication time. A total of 12 randomized experimental runs were

performed by taking particle size and percentage entrapment efficiency on the side of the response variable. The ANOVA model summary of particle size and entrapment efficiency was found to be significant ($p<0.05$) with R^2 of 86.71% and 95.68% respectively. The screening was done on the principle of Pareto chart i.e. 80% of problems come from 20% of the cause or 20% of invested input is responsible for 80% of the result obtained. From the screening design, three critical to quality factors were identified and further subjected to BBD optimization studies (Figure 5.15). The remaining two factors examined in PBD were set at a middle level as their effects on responses were statistically insignificant.

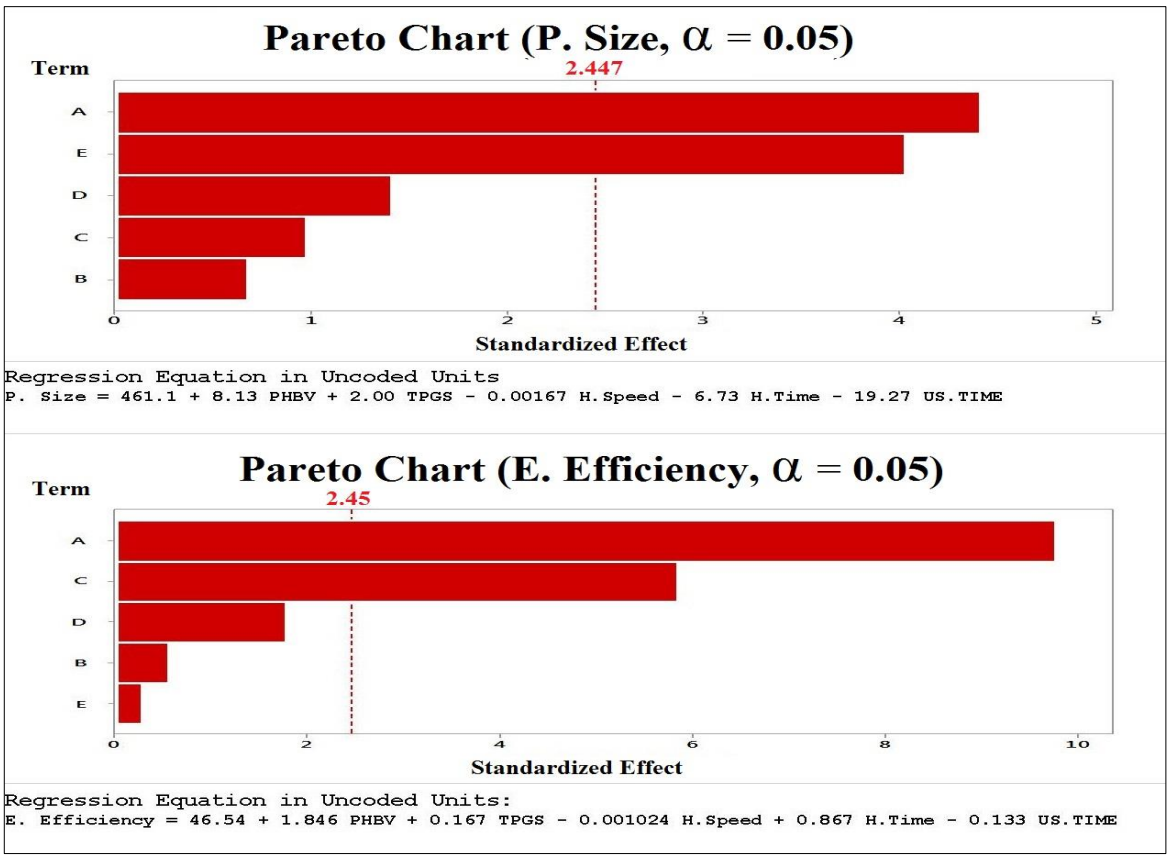

Figure 5.15 Pareto chart showing the influence of input variables on particle size and influence of input variables on entrapment efficiency

5.4.3 Box-Behnken design and statistical analysis

Formulation by design was carried out by RSM approach of 3 factors, 2 response, 3 level quadratic polynomial model Box-Behnken design using Design-Expert™ 10 software. A total of 17 runs were generated in a randomized fashion and experiments were performed by varying the levels of low (-1), intermediate (0) and high (1) combinations of each factor (Table 5.17). Each formulation was evaluated for particle size and percentage entrapment efficiency. The relative impacts of the independent variables on responses were compared by regression coefficient of coded factor equation. These mathematical equations were calculated by dividing the main effects by their standard errors. The positive and negative regression coefficient represents the synergistic and antagonistic effect of factors on selected responses.

Quadratic equation generated by BBD concerning coded factors fitting a polynomial function:

Particle Size = + 307.40 + 86.25* A - 4.62* B - 13.63* C - 2.50* AB - 0.50* AC + 1.25* BC - 1.58* A^2 + 15.17* B^2 + 10.68* C^2

E. Efficiency = + 65.40 + 13.12* A - 1.12* B + 1.75* C - 2.00* AB - 2.25* AC - 1.75* BC - 4.70* A^2 - 0.20* B^2 - 0.45* C^2

Analysis of variance study was done for the response surface quadratic model. The model results were found to be significant ($p<0.05$) showed the goodness of fit. The results obtained from ANOVA include F-value, *P*- value, lack of fit and R^2 implies the significant best-fit model for each response and is tabulated as a statistical summary of the model at 5% significant level (Table 5.18).

Table 5.17 Box-Behnken Design Matrix representing various combinations of independent variables and their observed responses

Run	PHBV (% w/v)	H. Speed (rpm)	US Time (min)	Particle Size (nm)	% E. Efficiency
1	2	4000	5.5	239	48
2	8.5	11000	5.5	323	62
3	8.5	11000	5.5	219	67
4	2	11000	3	243	43
5	8.5	11000	5.5	324	68
6	15	4000	5.5	410	78
7	15	11000	8	389	73
8	8.5	18000	8	318	65
9	8.5	4000	3	351	61
10	8.5	11000	5.5	328	59
11	15	18000	5.5	398	69
12	2	11000	8	211	51
13	15	11000	3	423	74
14	8.5	11000	5.5	343	71
15	8.5	4000	8	327	68
16	2	18000	5.5	237	47
17	8.5	18000	3	337	65

The interaction between process variables and product characteristics were demonstrated using two-dimensional contour (2D) and three-dimensional response surface (3D) plots (Figure 5.16). These plots are geometric illustration of selected responses over two independent variables which display the effect of increased or decreased levels of factors on the response. These plots demonstrate a quick visual guide to observing the effect of factors influencing response and allow us to understand the optimized formulation behavior. Desirability functional value of the process was found to be 0.856 showing good, desirable responses. Based on predicted optimization results the optimum levels of factors were generated for further optimization studies. The independent variables and the responses used in this statistical design along with their constraints predicted and experimental values are listed in Table 5.18.

Table 5.18 Independent and dependent variables with their levels, constraints, and goals in Box-Behnken design

Levels				
Independent variables (Factors)	**Low (-1)**	**Medium (0)**	**High (1)**	**BBD Results**
A. Polymer (%w/v)	2	8.5	15	10.83 mg
B. Homogenizer Speed (rpm)	4,000	11,000	18,000	4,962 rpm
C. Ultra Sonication Time (min)	3	5.5	8	8.39 min

Dependent variable (Response)	**Constraint**	**Predicted value**	**Experimental value****
Y_1 = Particle size (nm)	200-350	350	349±3.51
Y_2 = Entrapment efficiency (%)	Maximize	72.94	69±1.28

Statistical summary of model					
	F-Value	***p*-Value***	**R-Square**	**Lack of fit**	**Remarks**
Particle size	4.79	0.0255	0.8603	0.9951	Significant
Entrapment efficiency	11.17	0.0022	0.9349	0.8793	Significant

******p*-value < 0.05 was regarded as statistically significant; **Average of three determinations ±SD**

Finally, the optimized formulation with optimized levels of factors was prepared similarly as discussed in ‘formulation of docetaxel-loaded nanoparticles.' The experimentally obtained outcomes of optimized NPs are used to validate the predicted values of an optimized formulation. The validation of results was done based on the comparison of predicted and experimental values of optimized nanoparticles, and the percentage bias was found to be 0.2% for particle size and 0.05% for percentage entrapment efficiency. This close agreement between predicted and observed experimental results demonstrated the reliability of optimization procedure as per Box-Behnken design.

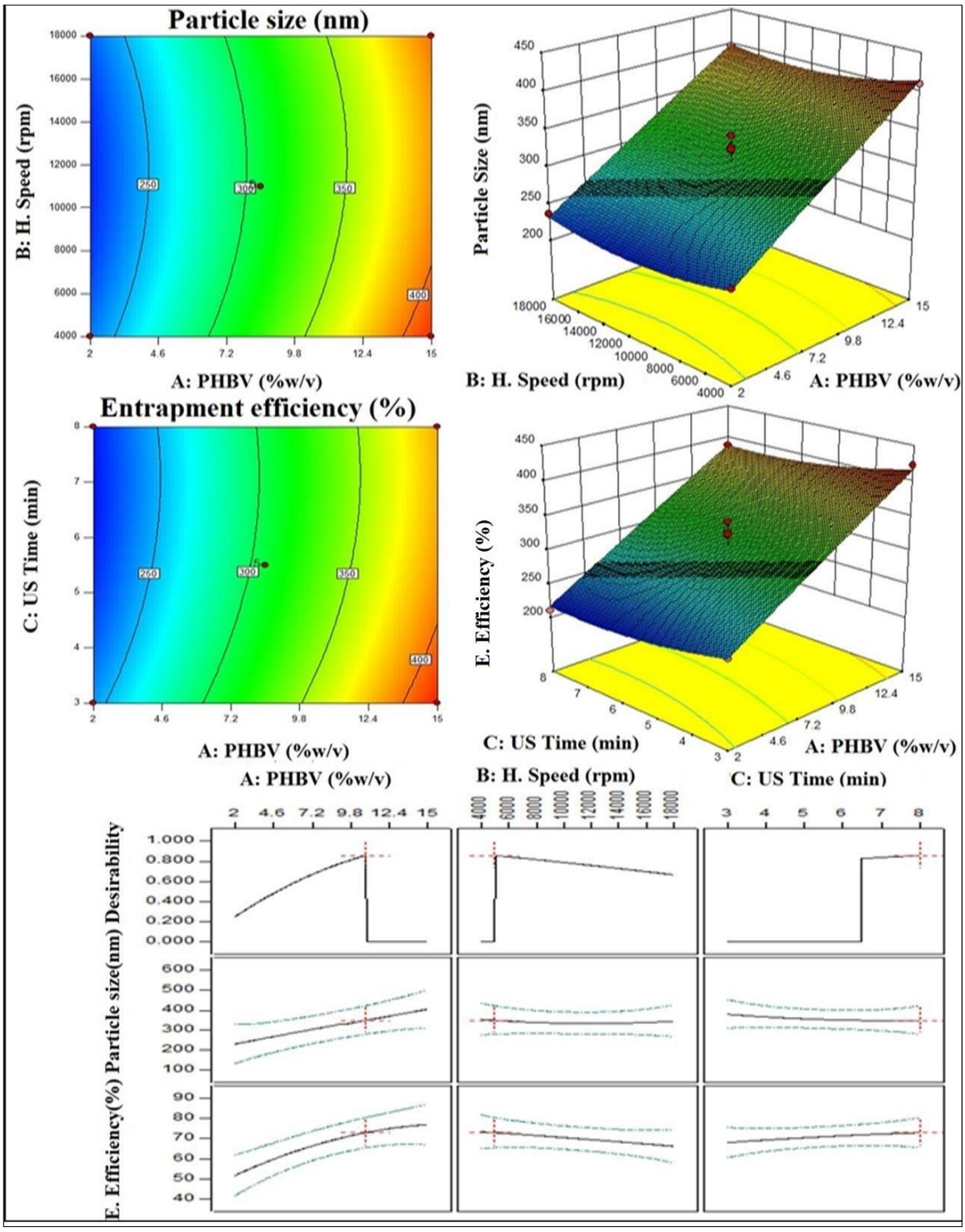

Figure 5.16 Contour, 3-D Response Surface Methodology and All factor plot showing the effect of independent variables on responses (effect of homogenizer speed and polymer concentration on particle size; effect of sonication time and polymer concentration on % entrapment efficiency)

5.4.4 Morphological study

The complete surface morphology of NPs was visualized by SEM, Carl Zeiss Inc., USA after the sample had been coated with gold using sputter coater. SEM images at different magnifications confirmed spherical nature of nanoparticles with a smooth surface without any aggregation or adhesion phenomena (Figure 5.17A). The AFM study was done with scanning probe microscope NT-MDT, Russia confirmed spherical nature of formulation without any aggregation and coalescence thereby providing stability to the colloid system (Figure 5.17B). TEM images of NPs were taken using TECHNAI-20G^2, Czech Republic showed the regular spherical shape, and uniform particle size which was in favorable agreement (Figure 5.17C). Some NPs depicted worm-shaped particles at initial stages of emulsification, followed by their breaking into smaller globules at the middle stage of emulsification. This closure analysis of TEM reveals that the particles were surrounded by a thick layer, hypothesized to be the TPGS which provides a mechanical barrier to prevent coalescence of the formed nanoparticles.

5.4.5 Average particle size, zeta potential, and pH value

Particle size and size distribution of prepared nanoparticles are of prime importance as it influences the drug release profile as well as extravasate the particles in tumor tissues by enhanced permeation and retention (EPR) effect. Nanoparticles ranging from 200-350 nm are considered to be fit for passive drug targeting. The size of optimized nanoparticles obtained after the aqueous dispersion was found to be 349±3.51 nm using Desla Nano-C, Beckman Coulter, USA. The Zeta potential is an

important parameter that demonstrates the aggregation behavior of prepared formulation. Zeta potential of optimized formulation was evaluated by Desla Nano-C, Beckman Coulter, and the values ranged between -14.8 to -17.6 mV. The negative value determines the long-term stability of formulation in colloidal system. Furthermore, the negative zeta potential of the system is not opsonized by the reticuloendothelial system (RES) and avoids sticking to the cell surfaces, thus can provide longer systemic circulation time.

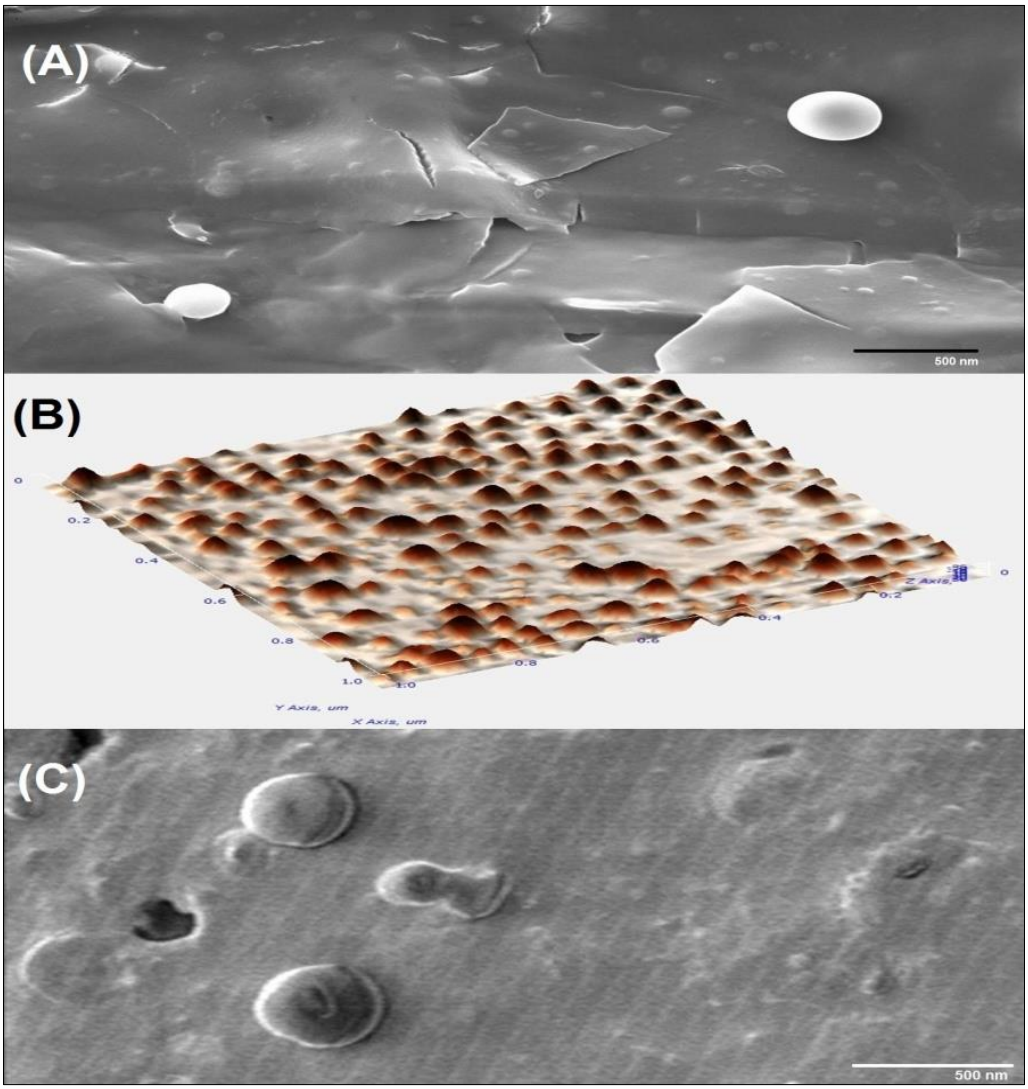

Figure 5.17 (A) SEM image; (B) AFM micrograph; (C) HR-TEM image of optimized nanoformulation

The pH of the formulation was found in the range between 5-8, indicated ideal for parenteral drug delivery [Date and Nagarsenker, 2008]. However, knowing that an extreme pH could be susceptible to the vein and RBC; the optimized formulation fulfilled the pH criteria required for intravenous administration.

5.4.6 In vitro drug release

In the preliminary stage of drug development, the release study is a crucial tool to perform measurement of drug availability and predict the extent of drug absorption. The drug dissolution and release are dependent on the physical retention and intra-particular pores of the polymeric nanoformulations. The drug release profile depicting a plot of cumulative percentage drug release versus time is shown in Figure 5.18. It was investigated using dialysis membrane in a non-biological system. The liberation of a drug from the optimized formulation exhibited a slow release about less than 10% drug release over a period of 48h and further delivered the drug with controlled rate, which is likely to be in support for prolonging the circulation of the formulation to meet EPR effect. The drug release mechanism was found to be the best fit for Zero order kinetics (R^2 = 0.969) model.

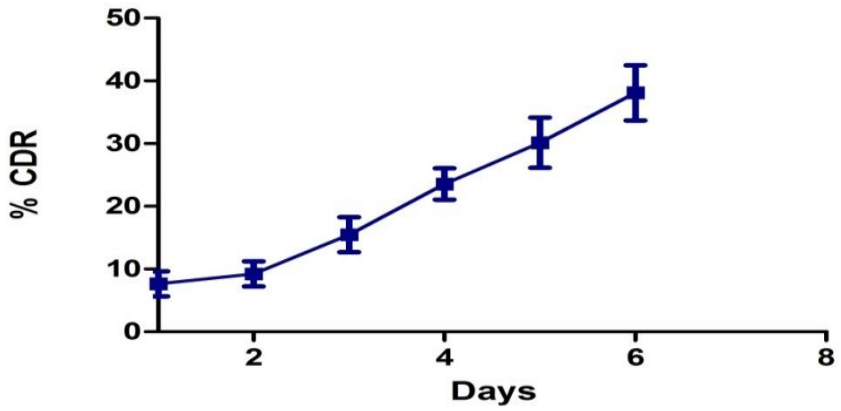

Figure 5.18 *In vitro* cumulative percentage of the drug release from PHBV NPs in PBS pH 7.4 (vertical bars represent average of three determinations ±SD)

5.5 Preparation of PHBV-PLH-PEG-DTX polymeric nanoparticles

5.5.1 Optimization and statistical analysis

Polymeric nanoparticles were subjected to optimization process by screening different factors using quality by design (QbD) systematic approach that emphasizes product and process quality. Its systematic approach includes defining quality target product profile (QTPP), setting up cause and effect diagram (Ishikawa diagram), control impact matrix (CIM), identifying critical quality attributes (CQA) including critical material attributes (CMA) and critical process parameter (CPP) relationship to CQA, risk assessment studies using failure mode effect & critical analysis (FMECA), screening important factors, implementing design of experiment utilizing Box-Behnken design (BBD) and validation of predicted and optimized test results [Vardhan et al., 2017b].

5.5.1.1 Quality target product profile (QTPP)

QTPP includes a well-organized summary of quality characteristics of formulations which ensure the quality, efficacy, and safety of the obtained optimized product [Rathore, 2009]. The elements of QTPP are used in the design criteria for the identification of CQA, CMA, and CPP (Table 5.19).

5.5.1.2 Box-Behnken design

BBD is a well-suited experimental design strategy that offers the possibility of investigating a high number of variables with only a limited number of experiments. The Box-Behnken design selected was a 15 randomized experimental runs with 3-factors, 2-responses, 3-levels to fit response surfaces using MODDE 12 software.

The statistical result of the test variables was based on the principle of quadratic process model and analysis of variance. The concentration of PHBV polymer (A), homogenizer speed (B), and ultrasonication time (C) along with the measured response values, expressed as mean particle size (Y1), and percentage entrapment efficiency (Y2) are presented in Table 5.20. These two responses were individually fitted to a quadratic process model and were then validated by ANOVA which was found statistically significant ($p<0.05$) and showed the goodness of fit. The results of ANOVA and lack of fit plots concerning error in the form of the histogram are shown in Figure 5.19.

Table 5.19 QTPP elements with their target

QTPP Elements	**Target**
Dosage form	Nanoparticle
Dosage design	Delayed control release
Therapeutic indication	Breast cancer
Drug targeting	Passive
Administration route	IV
Finished product	Lyophilized powder
Stability	6 months

Table 5.21 summarizes the factors and responses with their levels, constraints, and goal of the optimization process. The dynamic predicted set points profile of factors (independent variables) and predicted optimized results of response distribution plot obtained through MODDE 12 software are demonstrated in Figure 5.20. Three-dimensional response surface plots and two-dimensional contour plots were drawn

which visually demonstrated the effect of factors on responses. These plots give a clear idea about the effects of factors on the response before and after their corresponding optimized set points (Figure 5.21). Finally, the optimized experiment was conducted, and % bias was calculated by comparing the results of predicted and test results which were found to be within the limit i.e. < 2 demonstrated the reliability of optimization procedure (Table 5.21).

Table 5.20 Box-Behnken design matrix

Exp	PHBV	H Speed	Us Time	Particle Size	% E Efficiency
1	-1	-1	0	239	48
2	1	-1	0	423	72
3	-1	1	0	219	47
4	1	1	0	443	63
5	-1	0	-1	274	48
6	1	0	-1	460	78
7	-1	0	1	239	43
8	1	0	1	388	75
9	0	-1	-1	401	61
10	0	1	-1	378	69
11	0	-1	1	398	69
12	0	1	1	281	61
13	0	0	0	323	74
14	0	0	0	343	71
15	0	0	0	327	68

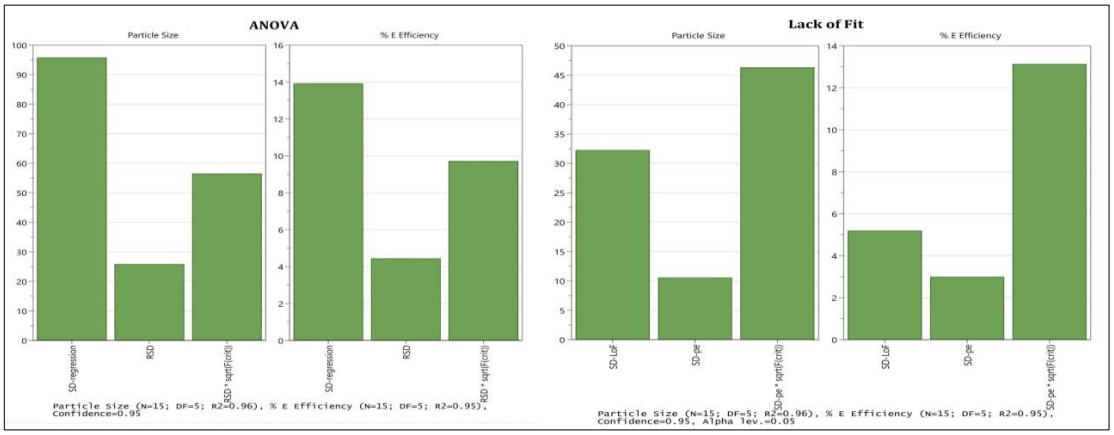

Figure 5.19 Analysis of variance and lack of fit plots with error showing goodness of fit for optimized process

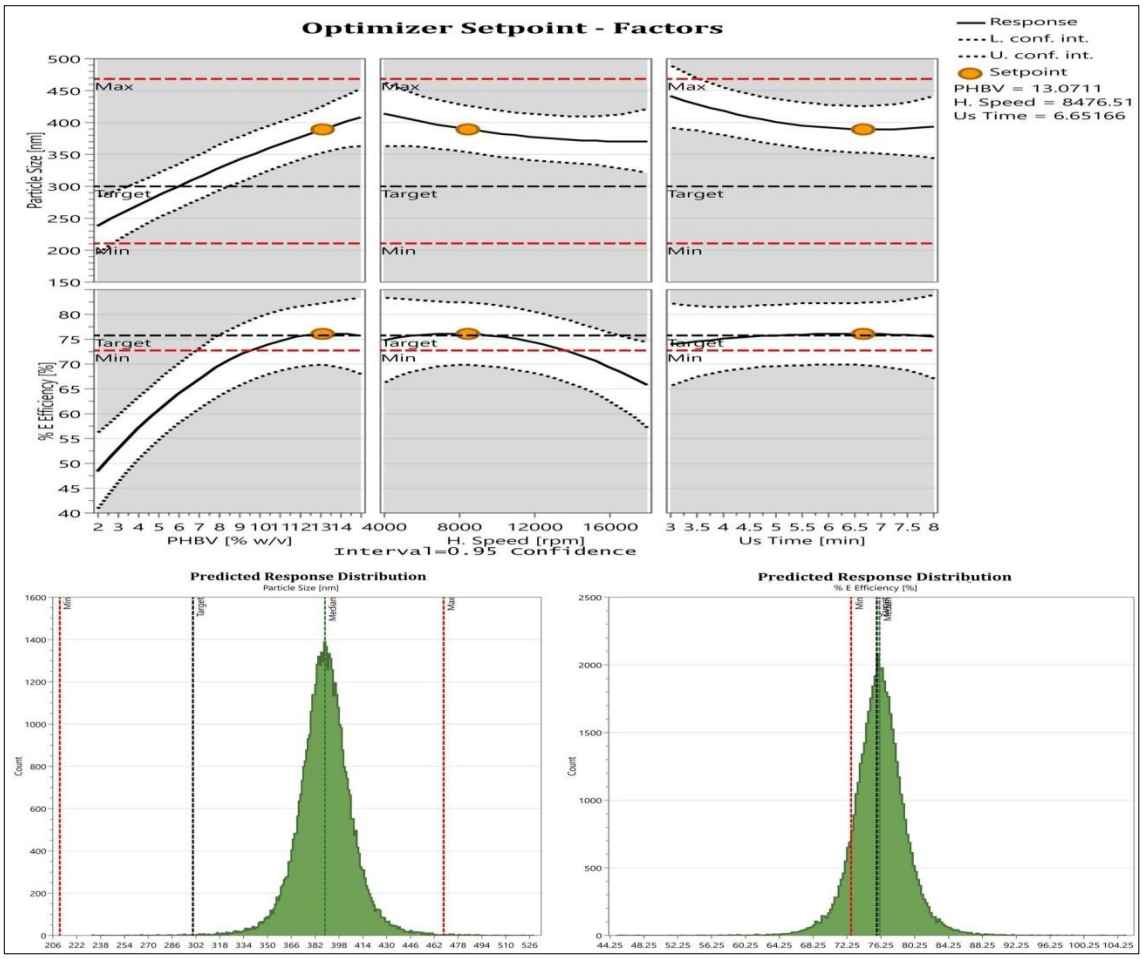

Figure 5.20 Optimized predicted set points of independent variables indicating the effect on particle size and entrapment efficiency and response distribution graph showing expected values of responses (particle size and entrapment efficiency)

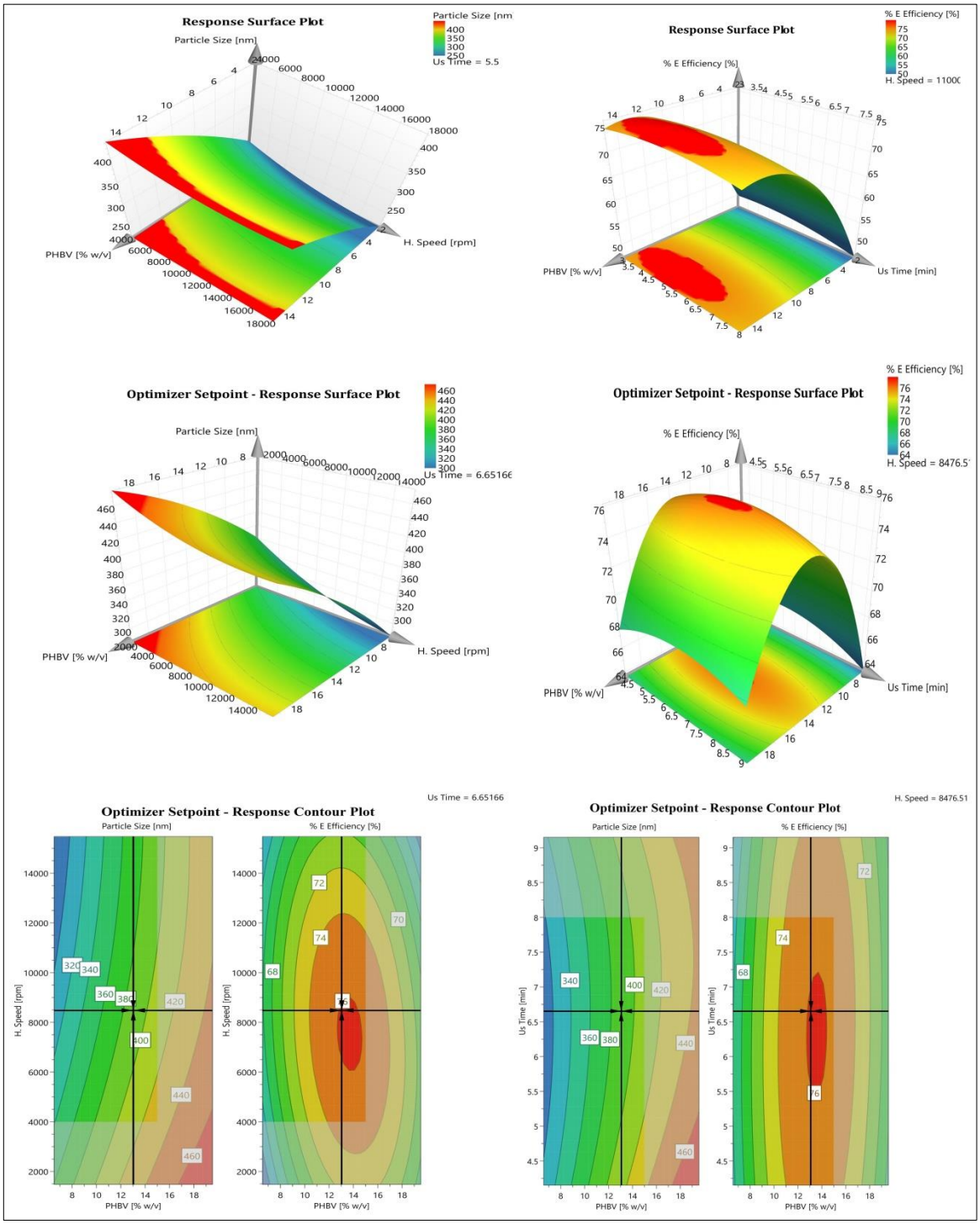

Figure 5.21 3-D response surface plot showing the effect on responses (effect of homogenizer speed and polymer concentration on particle size; effect of sonication time and polymer concentration on % entrapment efficiency) and contour surface plot showing the effects of independent variables on particle size and entrapment efficiency with their corresponding optimized set points

Table 5.21 Independent and dependent variables with their levels, constraints, and goal in Box-Behnken design

Levels Independent variables (Factors)	Low (-1)	Medium (0)	High (1)	BBD Results
A. Polymer (%w/v)	2	8.5	15	13.0711 mg
B. H. Speed (rpm)	4,000	11,000	18,000	8,476.51 rpm
C. US Time (min)	3	5.5	8	6.6516 min

Dependent variable (Response)	Constraint	Predicted value	Experimental value**
Y1 = Particle size (nm)	200-350	389.189	322±4.13
Y2 = E. efficiency (%)	Maximize	75.7625	67±0.91

Statistical summary of model	F-Value	*p*-Value*	R-Square	Lack of fit	Percentage bias
Particle size	13.721	0.0050	0.9610	0.0987	1.20%
E. efficiency	9.8021	0.0108	0.9463	0.2599	1.13%

***p*-value <0.05 consider as statistically significant; **Average of three determinations ±SD; f-value, fisher mean value; *p*-value, probability value**

The effect of parameters on particle size was found to be significant with an F value of 13.72 ($p<0.0050$), which indicates that response variable Y1 and the set of formulation variables were significantly related. The high R^2 value indicated that 96.10% of the variation in particle size was explained by the regression on formulation factors. The data indicated that the mean particle size was strongly dependent on the selected variables. In the case of entrapment efficiency, the optimized variables showed a good fit to the quadratic model with an F value of 9.80 ($p<0.0108$), which indicates that response variable Y2 and the set of formulation variable were significantly related. The high R^2 value indicated that 94.63% of the variation in %EE was explained by the regression on formulation factors. It has been shown that the maximum entrapment efficiency (67±0.91%)

with the desired particle size (322±4.13 nm) was achieved by using the optimal conditions of 13.0711 mg PHBV, homogenizer speed 8,476.51 rpm, and 6.65 min of ultrasonication time.

5.5.2 Average particle size, zeta potential, and PDI

The average particle size of optimized nanoformulation of DTX-PHBV-PLH-PEG (F4) was found to be 322±4.13 nm (Figure 5.22) as compared with the average particle size F1 (283±2.79 nm), F2 (260±2.85 nm) and F3 (349±3.51 nm). The pore cut-off size between cancer cells in the solid tumor is 380 to 780 nm. The sizes of formed nanoparticles between 200-300 nm are of prime importance for passive targeting to exploit EPR effect. When the concentration of surfactant increases the smaller size of particles were obtained, on the other hand, increased concentration of polymer lead to formation of larger particles. The average zeta potential of DTX-PHBV-PLH-PEG (F4) formulation -18±1.92 mV, F1 (-17±2.64 mV), F2 (-18±2.12 mV) and F3 (-16±1.36 mV) were found within acceptable limit indicating stability of nanoformulation as negative charge protect them from opsonization and prolong NPs circulation. A very low polydispersity index for F1 (0.143±0.11), F2 (0.212±0.14), F3 (0.134±0.10), and F4 (0.247±0.08) batches of nanoformulations was observed indicating a narrow size distribution of the nanoparticles and consequently a homogeneous distribution (Table 5.22).

Table 5.22 Different optimized formulations with their particle size, PDI and zeta potential

Formulation code	P. Size (nm)	PDI	Z. Potential (mV)
DTX-PHBV-PVA (F1)	283±2.79	0.143±0.11	-17±2.64
DTX-PHBV-PF127 (F2)	260±2.85	0.212±0.14	-18±2.12
DTX-PHBV-TPGS (F3)	349±3.51	0.134±0.10	-16±1.36
DTX-PHBV-PLH-PEG (F4)	322±4.13	0.247±0.08	-18±1.92

***Average of three determinations ±SD**

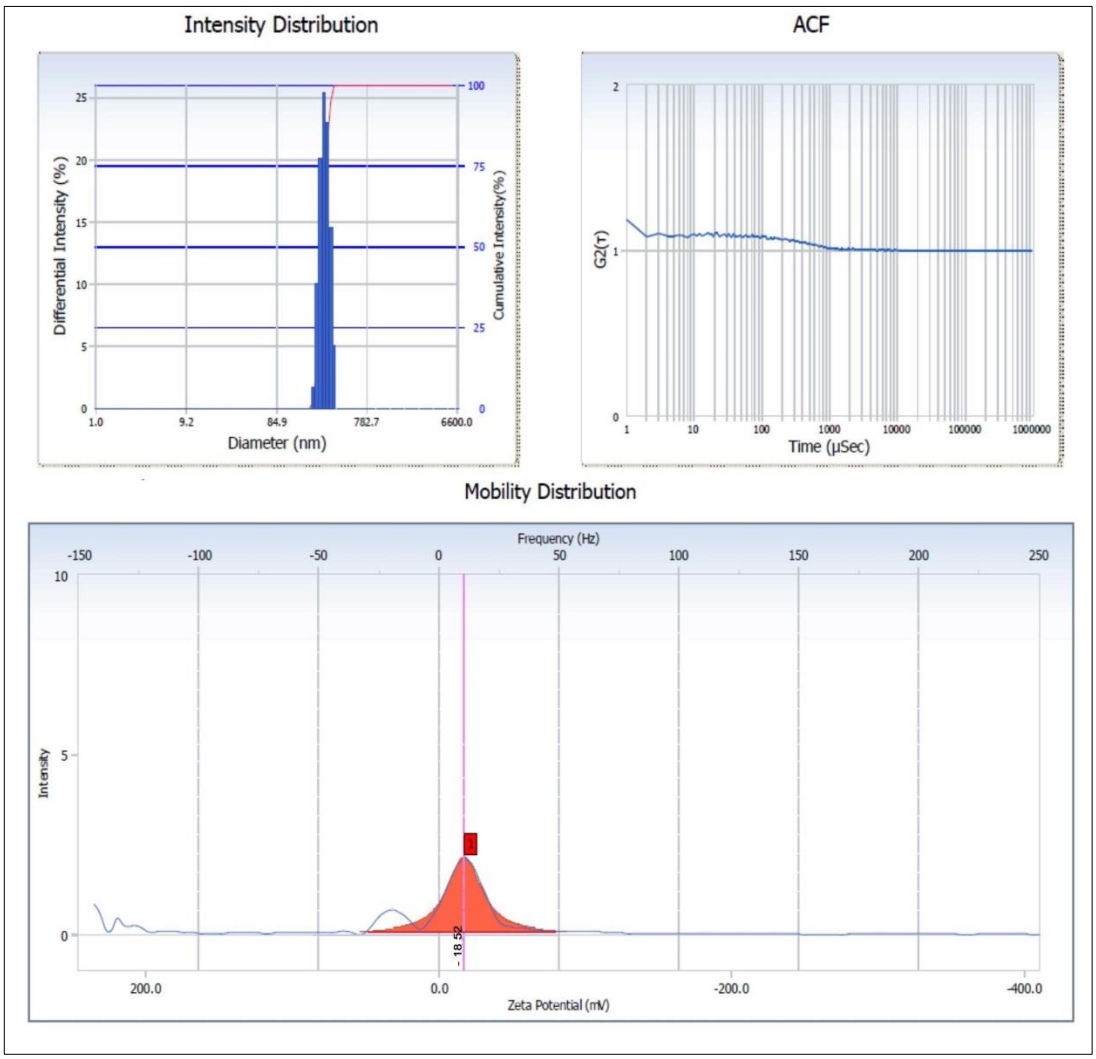

Figure 5.22 Results of particle size, PDI and zeta potential analysis for F4 optimized formulation

5.5.3 Entrapment efficiency

Figure 5.23 depicts the comparative histogram of particle size and % entrapment efficiency for all the nanoformulations. The entrapment efficiency of F1, F2, F3 and F4 formulations were found to be 44±0.59%, 39±0.85%, 69±1.28% and 67±0.91% respectively. High entrapment efficiency is advantageous since it carries adequate drug at the target site and increases the residence time of the drug [Rathore, 2009]. Thus, the order of %EE was found to be F3>F4>F1>F2.

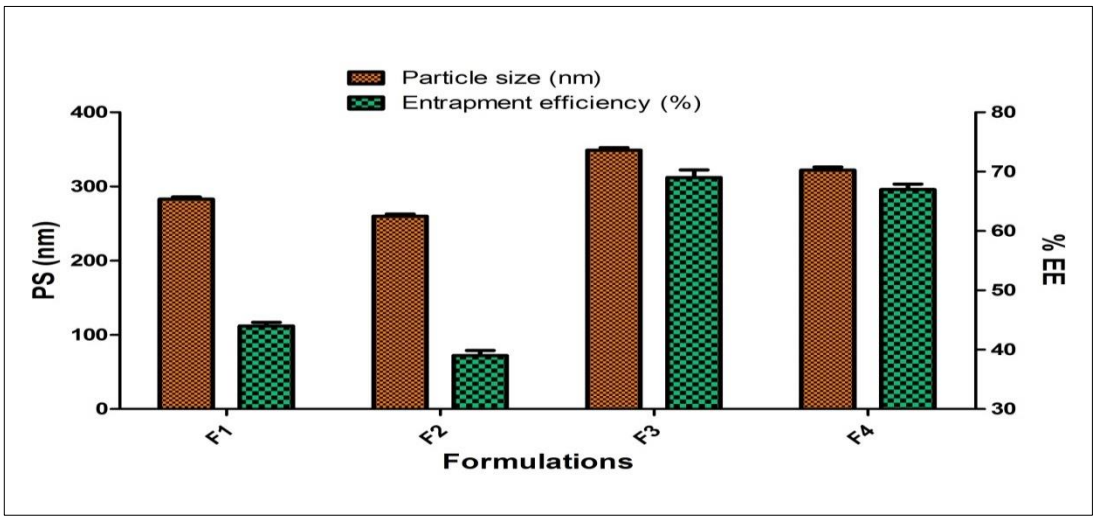

Figure 5.23 Multi y plot for percentage entrapment efficiency and particle size of different optimized formulations (vertical bars represent average of three determinations ±SD)

5.5.4 Surface morphology

The SEM, TEM and AFM micrographs of prepared nanoformulation revealed its exterior morphology, particle size, and distribution [Vardhan et al., 2017a]. In brief, the optimized nanoparticles were placed on a glass slide (SEM/AFM) or copper grid (TEM), air dried, further vacuum coated with gold (SEM) and finally examined for

surface morphology. It was evident by the photomicrographs that nanoformulations are in the range of preferred nano-size and having a spherical shape and smooth surface (Figure 5.24). The micrograph of AFM confirms that the nanoparticles were well dispersed without any agglomerates.

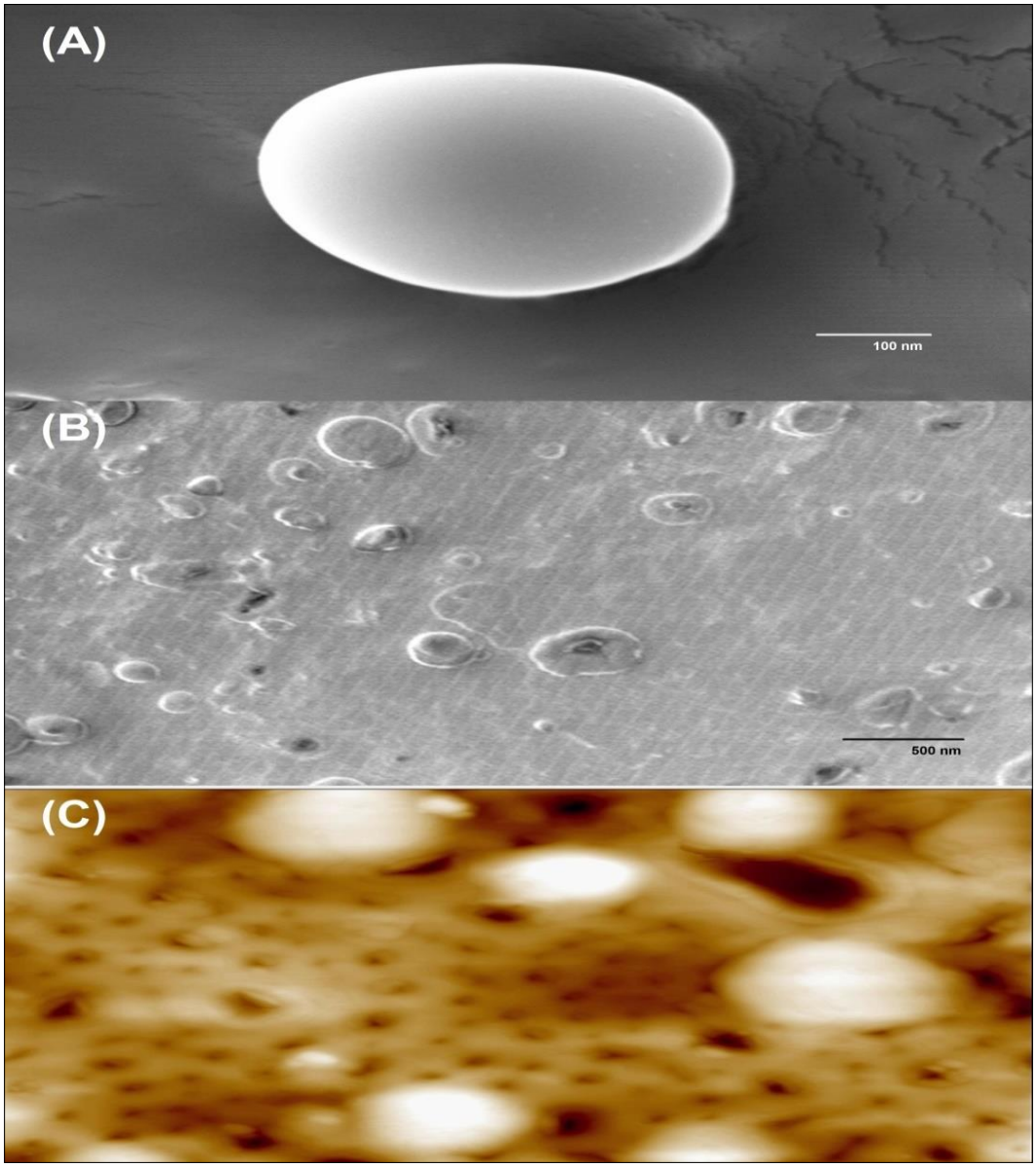

Figure 5.24 (A) SEM, (B) HR-TEM and (C) AFM micrographs of optimized nanoformulation

5.5.5 ^{1}H NMR spectroscopy

Proton nuclear magnetic resonance study was performed for DTX-PHBV-PLH-PEG (F4) formulation before and after the PLH-PE-PEG coating, and their spectra are shown in Figure 5.25. Prior to pegylation PHBV-TPGS NPs showed peaks at 2.08, 3.83, 4.22, 4.46 and 4.66 δ ppm. The absence -CH- peaks at 4.22, 4.46 and 4.66 δ ppm in final formulation showed evidence of complete pegylation. Thus, peaks and shifts of ^{1}H NMR spectrum of pegylated F4 gave strong proof for PLH-PE-PEG coating.

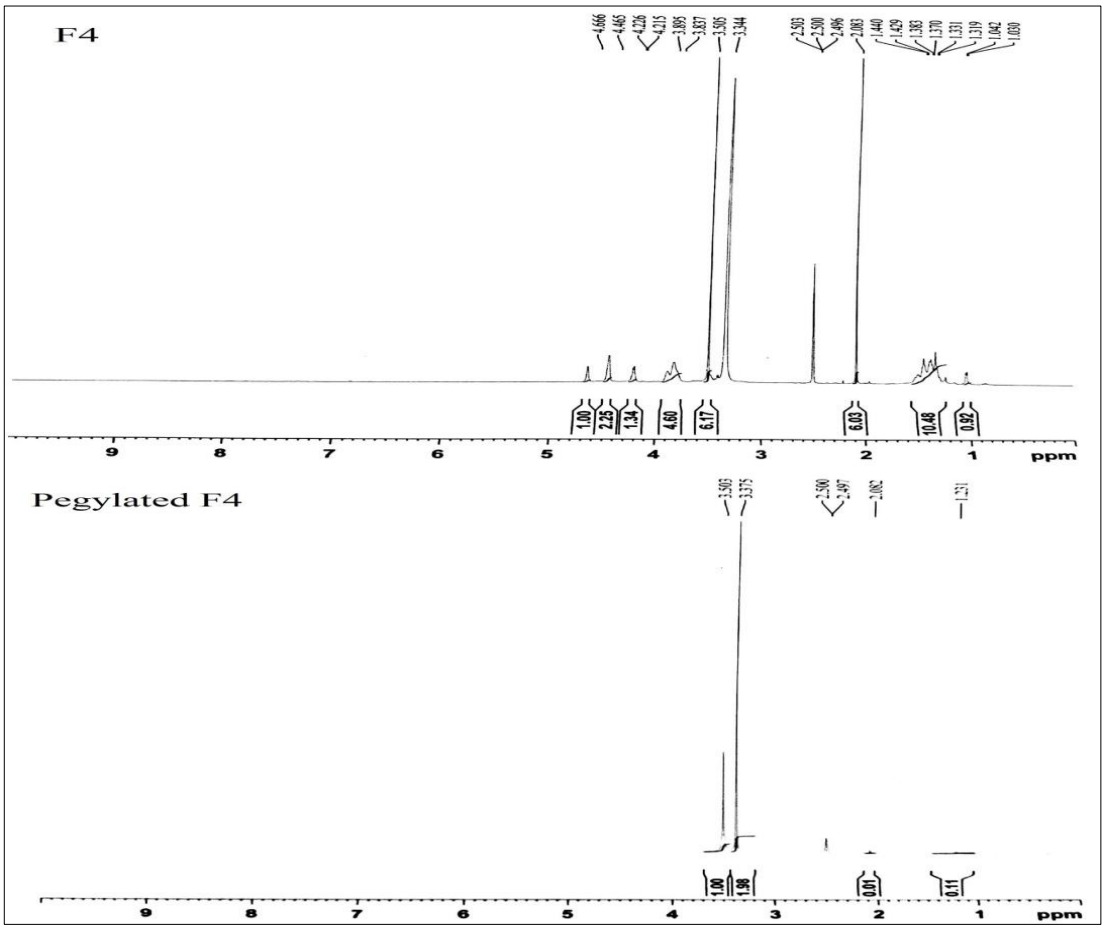

Figure 5.25 ^{1}H NMR spectra of F4 formulation before and after PLH-PE-PEG coating carried out in the pulsed FT mode at a 500 MHz resonance frequency for protons after dissolving samples in deuterated DMSO-d6

5.5.6 In vitro drug release studies

The drug release profile of all the formulations was performed in PBS pH 7.4 and the results obtained are shown in Figure 5.26. It was observed that the drug release involved no burst effect and was followed by slow drug release. About 20% of drug release was found for F2 and F3 whereas; around 10% of drug release was detected for F1 and F4 in four days' period. The study was conducted for six days, and results demonstrated release of drug in a controlled manner as per our goal.

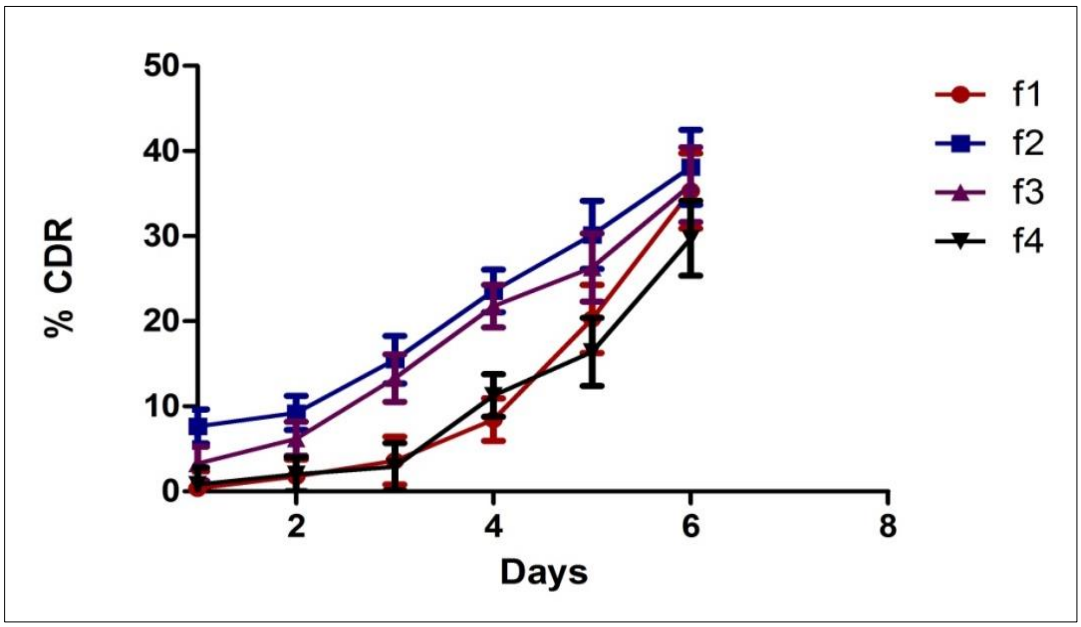

Figure 5.26 Cumulative percentage drug release versus time profiles of all the formulations (vertical bars represent average of three determinations ±SD)

Further, the release profile of docetaxel from DTX-PHBV-PVA (F1), DTX-PHBV-PF127 (F2), DTX-PHBV-TPGS (F3), and DTX-PHBV-PLH-PEG (F4) nanoparticles were examined by using different release kinetic models: zero order, first order, Higuchi and Korsmeyer-Peppas model, and their regression coefficient (R^2) were calculated. F1 followed the Korsmeyer-Peppas model (R^2-0.918) showed

an anomalous mechanism of drug release (n-0.6225) whereas other nanoformulations demonstrated zero order as their best fit model i.e. F2 (R^2-0.977), F3 (R^2-0.969) and F4 (R^2-0.875). Batch F4 exhibited maximum sustaining effect on drug release followed by batches F1, F3 and F2.

5.6 Drug excipient and drug plasma interaction study

The effectiveness, compatibility and physicochemical characteristics of drug and excipients were determined using Fourier transformed infrared spectroscopy (FTIR), X-ray diffraction (XRD), Differential scanning calorimetry (DSC) and SDS-PAGE. The degree of compatibility and interaction between drug and excipients used in the formulation may affect many of the performance related characteristics of the dosage form [Vardhan et al., 2017a].

5.6.1 Fourier Transform Infrared (FT-IR) spectroscopy

Fourier transform infrared spectroscopy (FTIR) studies investigate and predict any physicochemical interactions between components in the formulation and can, consequently, be applied for the selection of suitable chemically compatible excipients. FTIR instrument (SHIMADZU 8400, Japan) was used for compatibility study of the drug with different excipients by scanning over the wavelength range of 4000-400 cm^{-1}. Sample preparation involved mixing of potassium bromide with various samples in 100:1 ratio. The samples were powdered separately in mortar and pestle to form pellets under the hydraulic press. The overlays FTIR spectrums of all the optimized formulations along with the pure drug and PHBV are shown in Figure 5.27. If any interaction occurs, the spectra often lead to an identifiable change in

infrared profile. The FTIR spectrum of drug revealed characteristics absorption bands at 709 cm^{-1} (C-H bending), 1,109 cm^{-1} (C-O stretching), 1,497 cm^{-1} (C=C stretching), 1,711 cm^{-1} (C=O stretching), 2,979 cm^{-1} (C-H stretching), 3,437 cm^{-1} (NH stretching), and 3,480 cm^{-1} (O-H stretching). Also, a large number of characteristic bands were also observed in between 1500-500 cm^{-1} due to vibration of fingerprint region. The carbonyl band of polymer i.e. PHBV appears at 1,544 cm^{-1} and 1,175 cm^{-1} in the formulations. Overlapping of the CH stretching band of surfactant observed at 2,730 cm^{-1} and that of PHBV at 2,870 cm^{-1}. The formulation spectra showed retention and slight reduction of characteristic absorption of the drug due to loss of crystallinity. The presence of new absorption bands of the drug in formulations confirms that all the excipients used in the formulations have a compatible agreement with the drug and were encapsulated successfully [Gandhi et al., 2014, Mukhopadhyay et al., 2015].

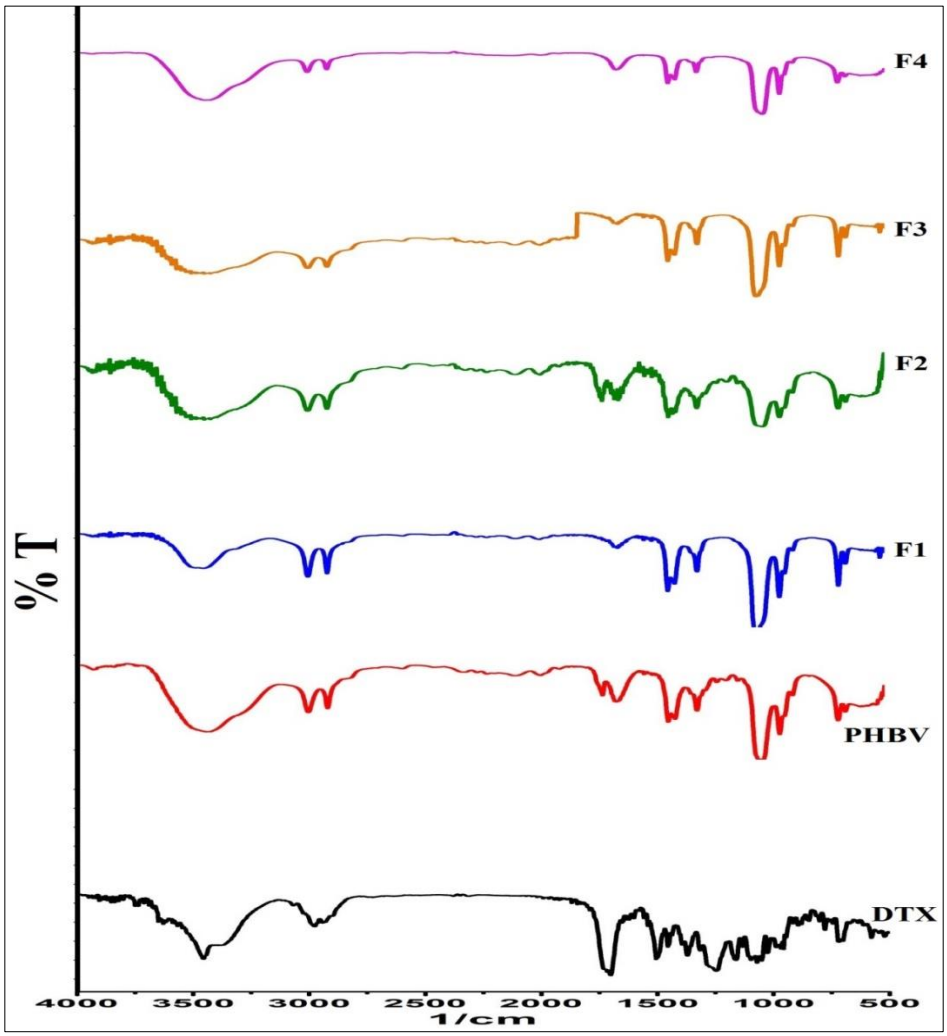

Figure 5.27 FTIR spectra of DTX, PHBV, F1, F2, F3 & F4 showing absorption bands

5.6.2 Powder X-ray diffraction (PXRD) study

X-Ray powder diffraction (XRD, Rigaku, Japan) technique is a family of non-destructive analytical technique which determines the type of polymorph or crystallinity present in the dispersion by providing structural data. PXRD is based on observing the scattered intensity of an X-ray beam falling on a specimen as a function of incident and scattered angle, polarization, and wavelength or energy.

XRD pattern was obtained using Ni-filtered Cu-K radiation at 45 kV and 40 mA at 2° min^{-1} scanning speed. XRD spectrums of the drug, PHBV, physical mixture (PM) along with optimized lyophilized formulations are shown in Figure 5.28, where Cu-Kα wavelength kept at 0.15405 nm. The study was recorded between 10° and 70° over the 2θ scanning range using the step size of 0.045° at 25 °C. The diffractogram confirmed the crystallinity of pure drug with sharp and distinctive peaks of 21.201, 25.423, 27.174, 29.842, 32.506, 37.283 and 40.203. Further, PHBV exhibited the characteristic peak at angles 39.2°, 44.1°, and 64.7° degrees. The XRD patterns in case of formulations resemble the absence of characteristic peak and were retained at reducing intensity thus, suggesting amorphous nature of the polymeric system.

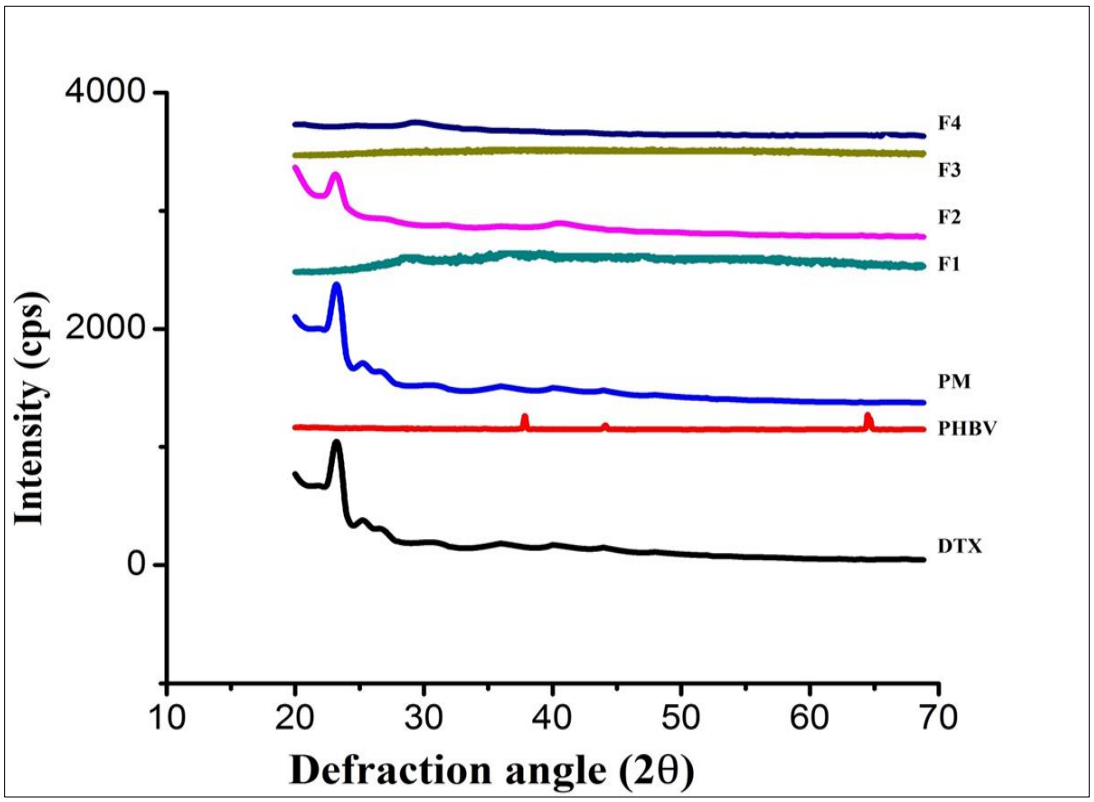

Figure 5.28 XRD analyses of DTX, PHBV, PM, F1, F2, F3 & F4 showing absorption bands

5.6.3 Differential scanning calorimetric (DSC) study

DSC was used to measure the endotherms or exotherms of the samples to know the physical and chemical changes in the formulation. Thermal analysis of drug and prepared formulations were carried out using DSC (TA Q1000, USA). Samples were weighed and placed in aluminum pans and heated 10-300°C with a heating rate of 10°C min^{-1} from ambient temperature. Thermal analysis of pure drug, PHBV, and prepared formulations are shown in Figure 5.29. Two sharp endothermic peaks of the drug at 169.49°C and 192.81°C indicated that the melting point of drug showing crystalline nature, whereas no distinct endothermic peak (melting peak of drug) was observed in the case of formulations therefore, signifying complete solubility of the drug in the polymeric system.

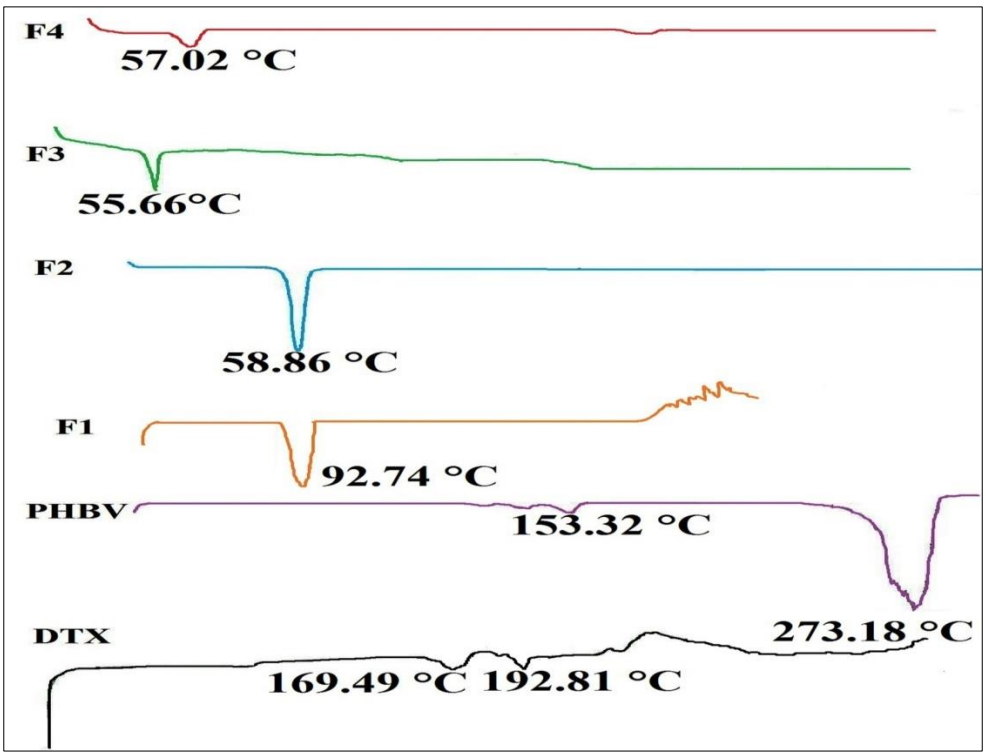

Figure 5.29 DSC thermograms of DTX, PHBV, F1, F2, F3 & F4 showing peaks

5.6.4 Interaction with rat plasma

Plasma protein absorption was performed by SDS-PAGE using Bio-Rad, USA electrophoretic apparatus [Vardhan et al., 2017b]. To identify and quantify proteins attached on the NPs surface, different concentration of rat plasma was mixed with prepared nanoformulations. The mixture was kept for overnight incubation at 37°C followed by centrifugation at 4000 rpm for 10 min. The results showed the absence of protein adsorption on optimized formulations by SDS-PAGE method (Figure 5.30). However, the free drug (D) was slowly released in the presence of plasma protein signifying strong drug-plasma binding. This little adsorption of plasma protein on optimized NPs surface helped to prevent opsonization.

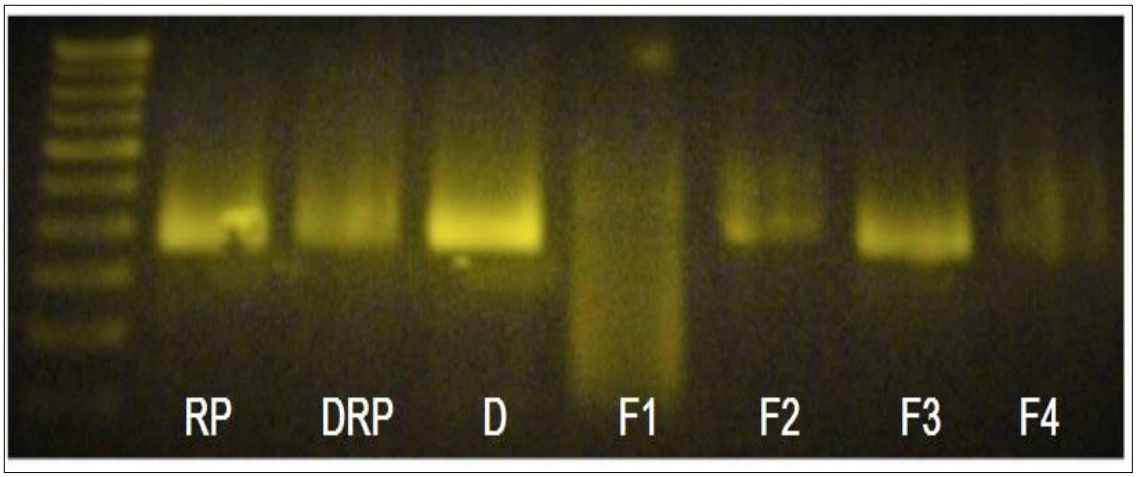

Figure 5.30 SDS-PAGE images of rat plasma with different optimized formulations along with rat plasma (RP), plasma containing drug (DRP), and free drug (D)

5.7 Cytotoxicity studies

Cytotoxicity study was done for the pure drug, optimized formulations and positive control (standard) to evaluate cell viability using sulforhodamine B assay [Adibkia et al., 2007, Vardhan et al., 2017a]. SRB assay was performed against human breast cancer cell line MCF7 to compare prepared nanoparticles with other different groups (pure drug, control, and standard) for percentage cell viability reduction. Cell growth was calculated by comparing the absorbance of treated versus untreated cells. The results of 50% inhibition of cancer cell growth were reported as GI_{50} values. Figure 5.31, gives a pictorial representation of significant reduction in cell viability of formulation treated groups in comparison to negative control MCF7 cell line observed under an inverted microscope and Figure 5.32 shows a graph representing percentage control growth versus concentration. The viability assay showed dye accumulation in dead cells however living cells were actively excluded from the dye. The GI_{50} values of 10µg/mL of the formulations were considered for the activity whereas percentage control growth inhibition was found in significant range. The results indicated significant potential to increase the cytotoxic effect. Therefore, the enhanced therapeutic efficacy of optimized nanoparticles was observed as compared to pure free drug and positive control groups. Formulation F4 offered maximum cell inhibition followed by F1, F2 and F3.

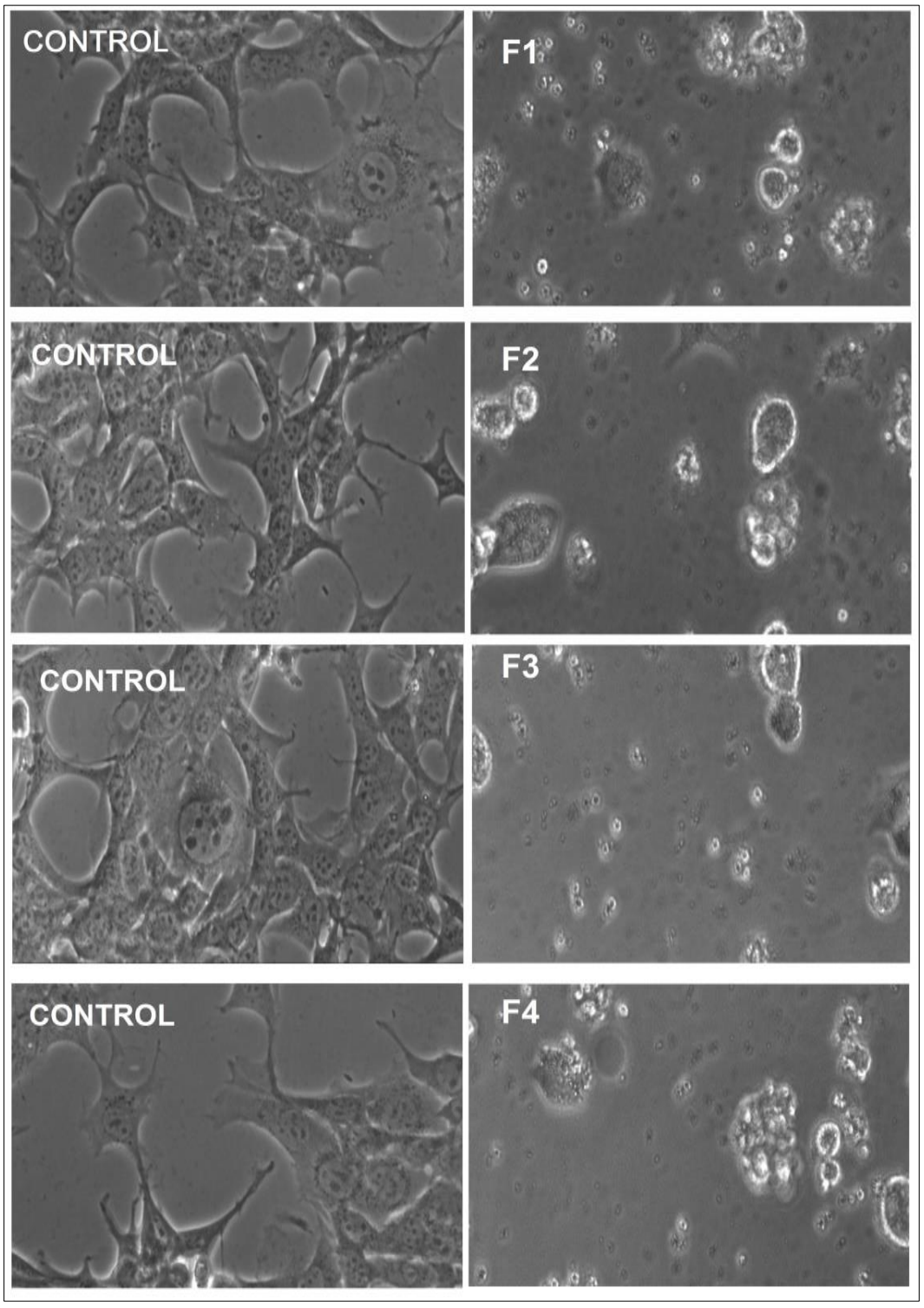

Figure 5.31 ***In vitro*** **cytotoxicity study of optimized nanoparticles with respect to their control observed under the inverted microscope in MCF7 cell lines**

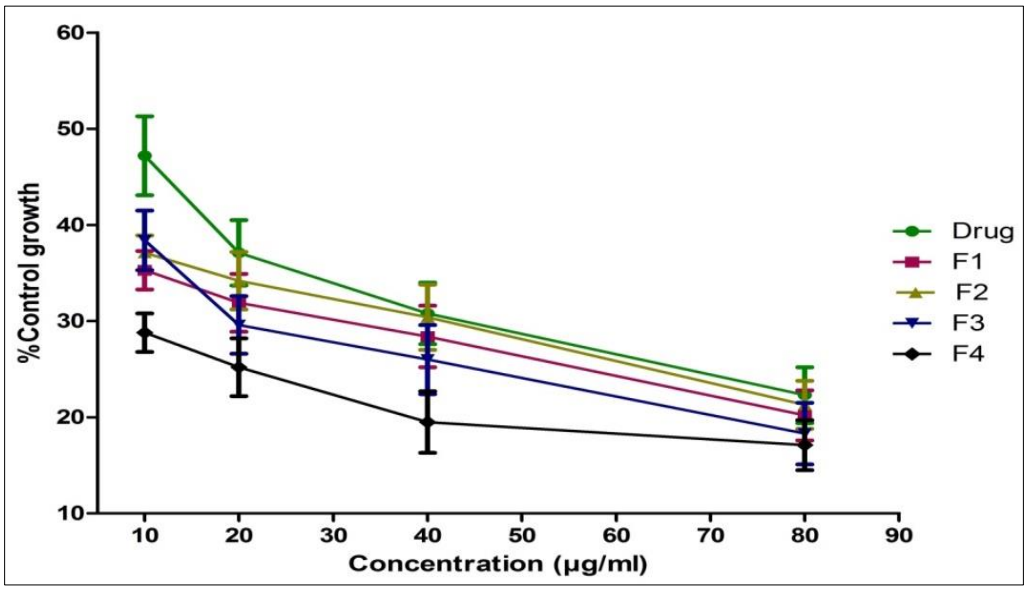

Figure 5.32 Percentage control growth versus concentration (µg/mL) profiles (vertical bars represent SEM; n=3; *p*<0.001 compared to pure drug; Two-way ANOVA: Bonferroni post-test)

5.8 Cellular uptake and cell viability studies

Internalization of developed formulations is an important and crucial factor for the success of targeted delivery systems as its success can demonstrate their therapeutic efficacies through intracellular release [Liu et al., 2013]. For cell uptake experiment, MCF7 cell lines were treated with nanoformulations tagged with fluorescent dyes (fluorescent isothiocyanate), and the percentage uptake was evaluated. Fluorescent labeled nanoparticles showed an increase in cell internalization after 48 h of treatment. The confocal microscopy image of optimized formulations shows fluorescent signals confirming the intracellular uptake which was observed within the cytoplasm of MCF7 cells (Figure 5.33A). For cell viability study, rat lymphocytes were maintained in DMEM, 10% FCS and 5% CO_2 at 37 ^{0}C in a 96 well plate. The cells (3500 cells/well) were treated with 10 µg/mL of test

formulation, untreated wells received an equivalent amount of PBS pH 7.4 and incubated for 24 h. Post-treatment 20 µL of cell suspension was diluted with equal amount of trypan blue and observed under the microscope. Blue cells represent dead cells, and transparent cells represent viable cells. In Figure 5.33 (B) no blue-stained cells were observed which confirms no apparent cytotoxicity at the concentrations tested.

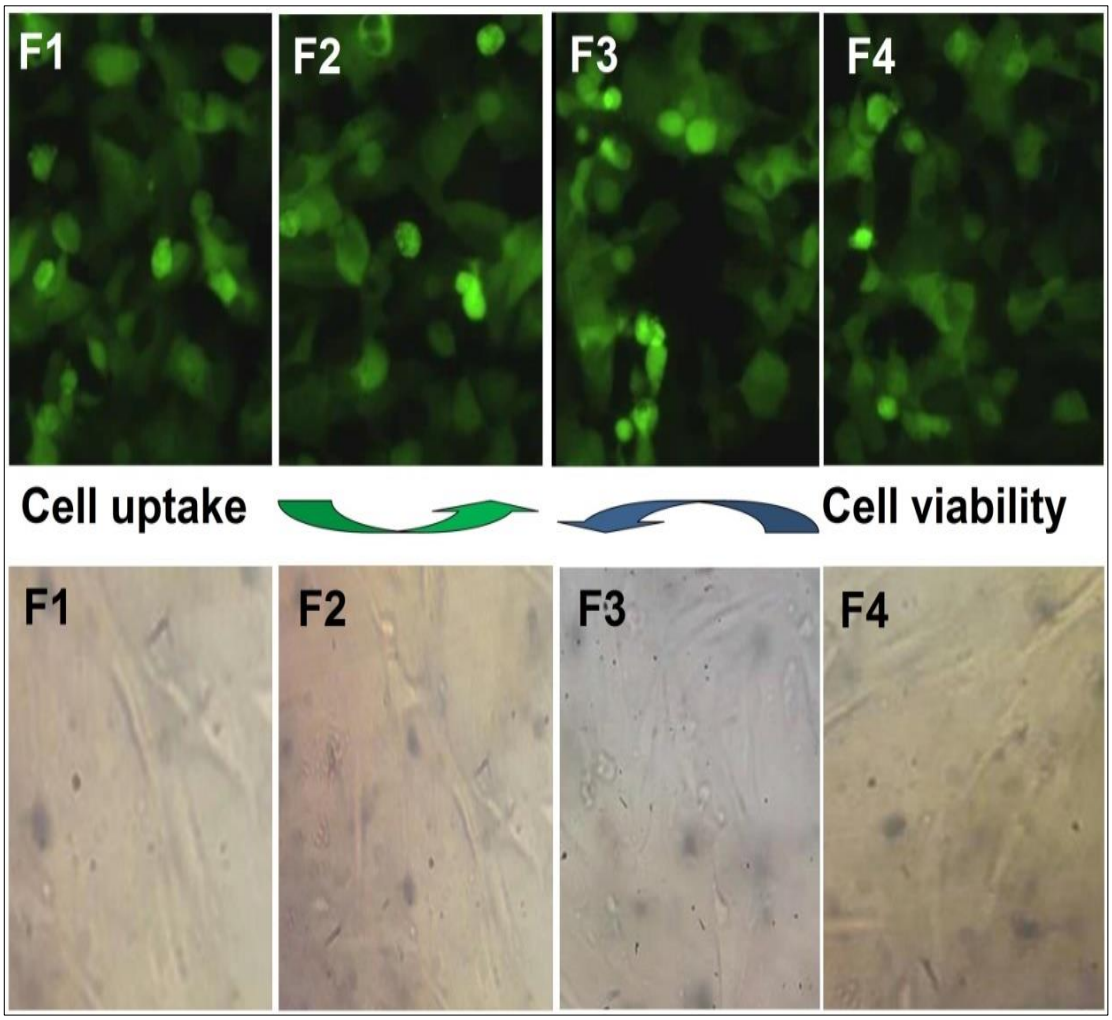

Figure 5.33 (A) Intracellular uptake of formulations tagged with dye (FITC) demonstrated by confocal microscopy imaging; (B) photographs representing trypan blue assay on rat lymphocytes for cell viability studies

5.9 Evaluation of hemolysis and platelet aggregation

For every intravenous formulation, the evaluation of hemolysis is mandatory. An *in vitro* hemolysis study is performed for the drug and excipients intended for injectable use in order to test and determine hemolytic potential [Dobrovolskaia et al., 2008]. Here, the blood sample of the rat was collected, centrifuged (4000 rpm for 10 min) and erythrocyte pellets were mixed with optimized formulations. The RBC suspension with nanoformulations was incubated (45 min at 37°C), diluted and dropped to a glass slide to make blood smears. The observed optical microscopic images of RBCs through Dewinter microscope demonstrated the absence of hemolysis in the case of optimized NPs, making them as an appropriate candidate for the application (Figure 5.34). In this study, the percentage hemolysis was found to be within recommended limit as per international standard (1% US FDA and 0.8% Council of Europe guideline) throughout the study period which confirmed its safety and compatibility (Figure 5.35). In the case of platelet aggregation study, rat blood (2 mL) was collected and same procedure as for hemolysis was followed for erythrocytes separation. Nanoformulations and erythrocytes with pH 7.4 PBS were incubated for 2 h. The formed suspension was diluted and kept on the orbital shaker. The blood smear was prepared on glass slides and qualitatively analyzed with the help of optical microscope (Figure 5.34). All the optimized formulations were found safe for intravenous administration as no significant platelet aggregation occurred at the concentrations tested.

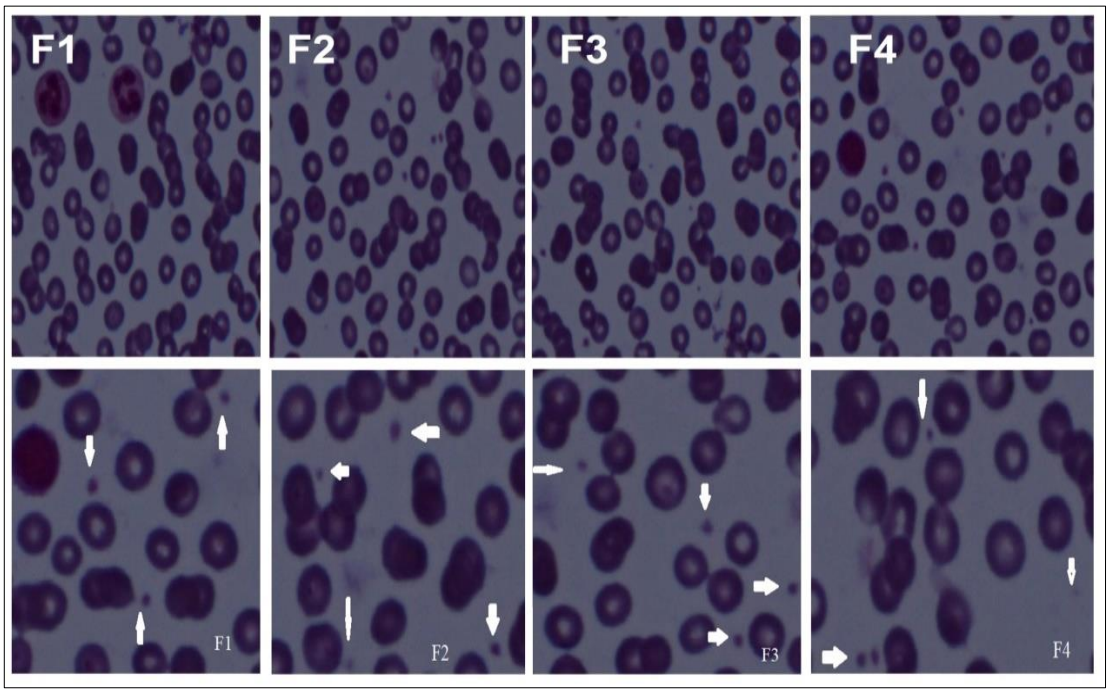

Figure 5.34 Image of red blood cells (RBC) observed after hemolysis and platelet aggregation studies by optical microscopy

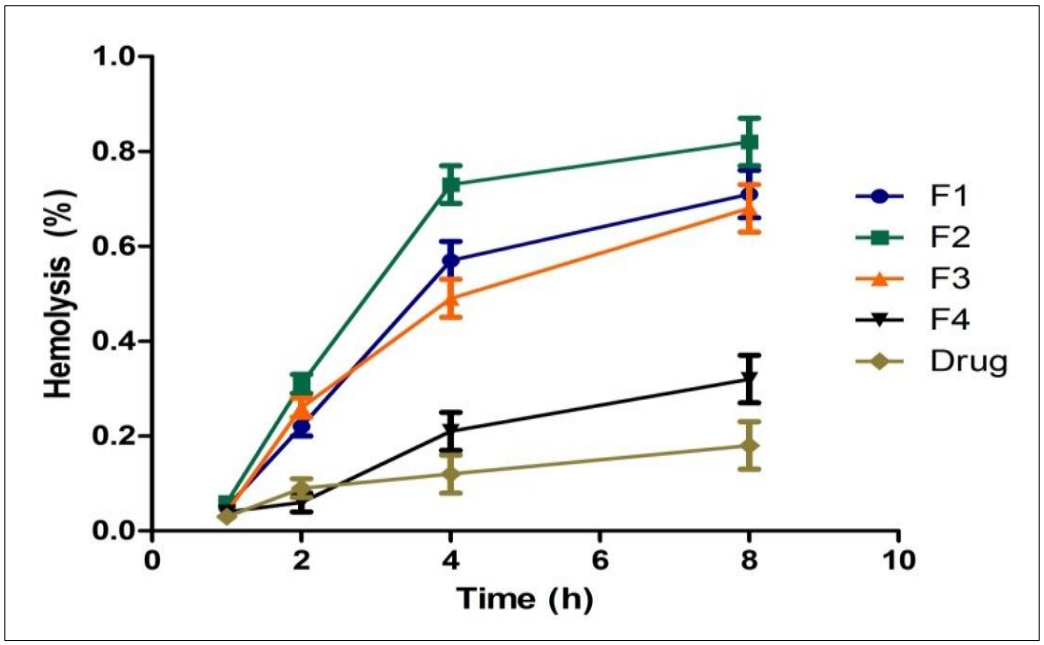

Figure 5.35 Percentage hemolysis against time (h) upon i.v. administration (vertical bars represent SEM; n=3)

5.10 Pharmacokinetic studies

Pharmacokinetic analysis is mainly used to estimate PK parameters and for measurement of bioavailability [Vardhan et al., 2017b]. The mean plasma concentration-time profile of the pure drug and drug loaded optimized formulations are illustrated in Figure 5.36 and their pharmacokinetic parameters ($C_{max,}$ $T_{max,}$ AUC_{0-t}, MRT, $T_{1/2,}$ & CL) in Table 5.23. The *in vivo* studies distinctly revealed that the pharmacokinetics and biodistribution of docetaxel were significantly altered when delivered in the form of PHBV nanoparticles. Plasma concentration-time profile and pharmacokinetic data indicate that the free drug solution rapidly cleared off from the blood circulation and was detected only till the 24 h following single i.v. administration. The pharmacokinetic study, *in silico* pharmacokinetic predictions and IVIVC of the formulation, were performed using different modules of GastroPlus™ software. The non-compartmental analysis of pure drug and developed nanoformulations were performed using PKPlus™ module of GastroPlus™. The C_{max} of optimized formulation was 1.8 (F1), 2.6 (F2), 2.5 (F3) & 2.8 (F4) times lower than that of pure drug suggesting reduced intensity of adverse effects related to high dose. Higher AUC_{0-t} 3.8 fold (F1), 3.9 fold (F2), 4.3 fold (F3), 4.7 fold (F4); higher $T_{1/2}$ 5.6 fold (F1), 8.2 fold (F2), 7.8 fold (F3), 9.4 fold (F4); higher MRT 10.9 fold (F1), 13.1 fold (F2), 14 fold (F3), 16 fold (F4); and lower CL_{tot} 3.9 (F1), 4.1 (F2), 4.3 (F3), 4.8 (F4) times were obtained from optimized formulations compared to pure drug suspension implying longer retention in the circulatory system.

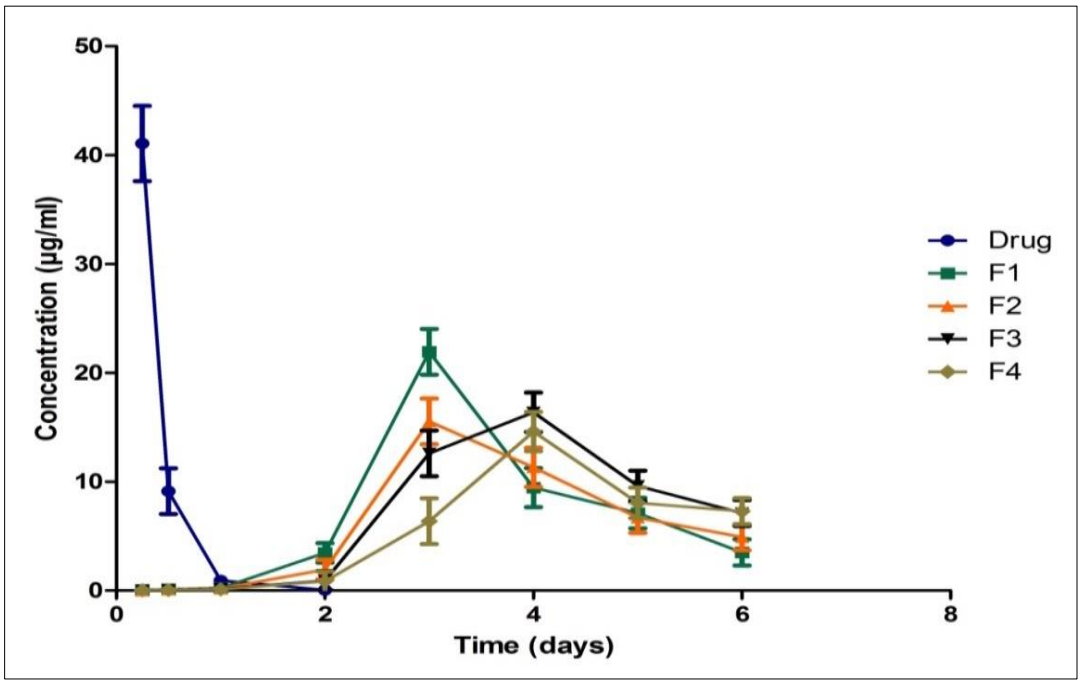

Figure 5.36 Plasma drug concentration-time profiles of pure drug and prepared formulations (F1, F2, F3 & F4) following i.v. administration in rats (vertical bars represent SEM; n=6; *p*<0.05 compared to pure drug; One-way ANOVA: student's t-test)

Thus, the mean resident time in pharmacokinetic studies was found to be in the order of F4>F3>F2>F1 i.e., F4 retained for much longer duration and F1 for less duration. Higher AUCs demonstrated an enhancement in relative bioavailability of nanoformulations. Overall improved pharmacokinetic profile of formulations could be due to the stealth associated negative charge that helps to escape the opsonization process during blood circulation. Statistical evaluation by student's t-test ($P<0.05$) revealed a significant statistical difference between drug suspension and optimized formulations for all the parameters.

Table 5.23 Pharmacokinetic parameter (non-compartmental) calculated through PKPlus™ software

Parameter	Drug	F1	F2	F3	F4
C_{max} (µg/mL)	41.06±2.81	21.93±1.31	15.53±0.96	16.38±0.82	14.61±0.21
T_{max} (h)	6±0.13	72±0.11	72±0.12	96±0.09	96±0.17
AUC_{0-t}(µg-h/mL)	301.7±17.81	1173.7±47.21	1202.5±52.35	1303.5±49.53	1440.6±86.91
$t_{1/2}$ (h)	5.09±0.13	28.77±1.92	41.80±2.75	40±3.65	47.85±2.86
MRT (h)	9.07±0.64	99.36±3.82	119.46±7.81	127.43±5.98	144.71±9.73
CL (L/h)	0.082±0.33	0.021±0.21	0.020±0.16	0.019±0.36	0.017±0.32
***In silico* parameter (GastroPlus™)**		**SF & (FE)**	**SF & (FE)**	**SF & (FE)**	**SF & (FE)**
AUC_{0-t}(µg-h/mL)		1180.5 (1.00)	1102.4 (1.09)	1421.6 (1.09)	1572.5 (1.09)

Values indicate mean (n=6) ± SEM; AUC, area under curve; MRT, mean resident time; SF, simulated formulation; FE, fold error

5.11 In silico prediction and in vitro-in vivo correlation

Since, through pharmacokinetic study, the optimized formulation proved their ability of enhanced bioavailability in rats, an effort was made to obtain an *in silico* prediction of their plasma concentration-time profile and pharmacokinetic parameters. GastroPlus™ software was utilized for *in silico* pharmacokinetic predictions of the observed and simulated profiles of optimized formulations [Vardhan et al., 2017b]. All the required parameters (Molecular weight, solubility, log *P*, dosage form, mean precipitation time, diffusion coefficient, drug particle density, rat body weight, CL, V_c, C_{max}, T_{max}, and AUC) were fed into the compound and pharmacokinetics tab, and outcomes of simulation observed. The observed and

predicted plasma concentration-time profile was found to be non-superimposable as shown in Figure 5.37, but its prediction accuracy can be established by fold error. The resultant fold error < 2, signify good prediction accuracy for the system as shown in Table 5.23. IVIVC was established to obtain the relationship between *in vitro-in vivo* correlation of drug release and pharmacokinetic data [Vardhan et al., 2017b]. Here, deconvolution was performed which is a calculation of cumulative *in vivo* absorption rate from plasma concentration-time data by mechanistic absorption model. The *in vitro-in vivo* correlations were established by IVIVCPlus™ module, and Single Weibull function of the mechanistic model was chosen to describe the *in vitro-in vivo* correlation which was found to be in limited correlation (Figure 5.38). Thus, the ability of the model to predict *in vivo* behavior of PHBV NPs from *in vitro* release studies was verified indicating non-linear relationship (limited correlation).

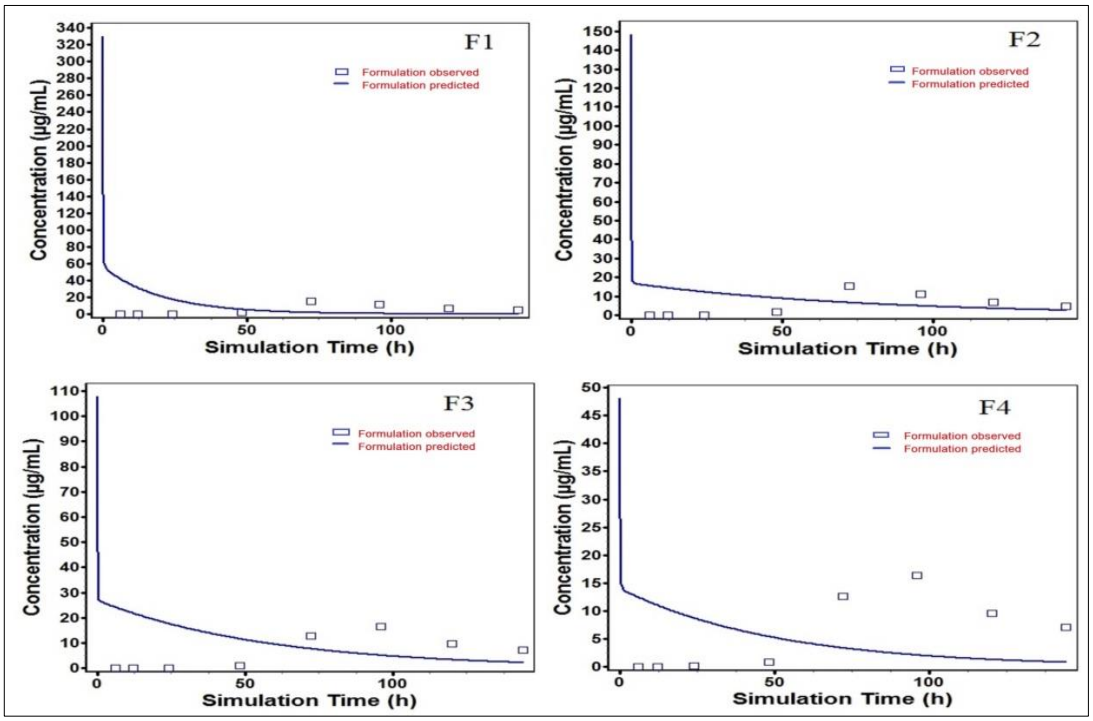

Figure 5.37 Experimental and simulated plasma concentration-time profile of optimized formulations

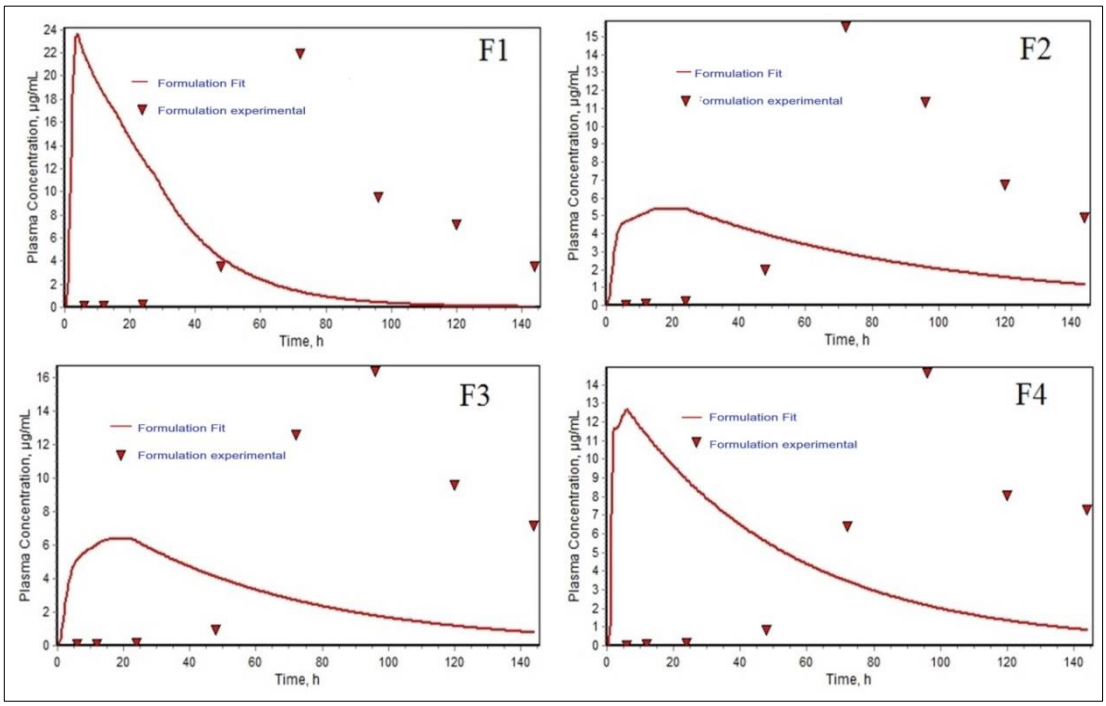

Figure 5.38 Observed *in vitro- in vivo* correlation of drug loaded optimized formulations

5.12 In vivo anticancer activity

In vivo activity on murine tumor model using C3H/J Mammary strain of female mice (6 mice in each group) was done for 30 days [Vardhan et al., 2017b]. All 42 female mice were fed regular diet and were incubated with C3H/Jax murine breast cells. The tumor bearing control (saline only), standard (doxorubicin), pure drug (docetaxel) and prepared formulations (F1, F2, F3 & F4) were injected through the i.v. route (tail vein) to the mice and efficacy of optimized formulations along with weight loss, tumor volume, and mortality parameters were recorded. Intravenous dose calculation was done utilizing maximum tolerated dose evaluation (MTD). 100 mg/Kg was considered as the final optimized dose for each mice per month i.e. 25 mg/Kg once a week for four weeks (Table 5.24). A significant anticancer efficacy

was observed for all the groups in comparison with control group. Figure 5.39 (A) shows safety profile of nanoparticles representing changes in body weight on days. A slight increase in body weight was witnessed with the standard, pure drug, and optimized formulations. The weight loss in case of optimized nanoparticles was found to be < 4 grams/mice indicated no toxicity within the experimental term. Optimized formulations in comparison to pure drug and standard exhibited a significant increase in body weight in the order of F4>F3>F1>F2>DTX. The relative tumor volume data represented a close agreement to the optimized formulations, which was able to significantly inhibit the tumor area as compared to other groups in order of F4>F3>F1>F2>STD>DTX>Control (Figure 5.39B). On the contrary, a continued increase in the tumor volume of the control group was observed. Figure 5.40, showed photographs of tumor-bearing mice at different experimental end points treated with the optimized formulations as an evidence of treatment efficiency. Kaplan-Meier survival data was plotted to check the survival of animals used in the treatment with control, standard, pure drug, and optimized formulations (Figure 5.39C). The 100% survival was recorded on behalf of optimized formulations, pure drug, and standard throughout the experimentation period. The *in vivo* activity results might be explained the increased local concentration of optimized formulation in the tumor tissues favored by EPR effect and longer plasma circulation time. Thus, the efficacy study of optimized formulations showed a positive evidence of effectiveness for the treatment of solid tumors. Figure 5.39 (D) represents T/C values Vs days demonstrated significant activity of optimized nanoparticles (T/C<0.4) over pure drug and standard groups in order of F4>F3>F1>F2>STD>DTX. By considering overall plots of all the graphs, it

can be concluded that the optimized formulations had significant superiority over all other groups in suppressing tumors.

Table 5.24 Maximum tolerated dose evaluation

Drug	Dose used	Mice dead	% Death	Wt. loss (>4 gm)	Toxicity criteria	MTD Further
F1	50 mg/Kg	0/6	0	No	Well tolerated	100 mg/Kg
	100 mg/Kg	0/6	0	No	Well tolerated	150 mg/Kg
	150 mg/Kg	0/6	0	No	Insoluble	100 mg/Kg
F2	100 mg/Kg	0/6	0	No	Well tolerated	150 mg/Kg
	150 mg/Kg	0/6	0	No	Insoluble	100 mg/Kg
F3	100 mg/Kg	0/6	0	No	Well tolerated	150 mg/Kg
	150 mg/Kg	0/6	0	No	Insoluble	100 mg/Kg
F4	100 mg/Kg	0/6	0	No	Well tolerated	150 mg/Kg
	150 mg/Kg	0/6	0	No	Insoluble	100 mg/Kg

***150 mg/Kg dose was found to be insoluble and thus can't be injected (i.v.)**

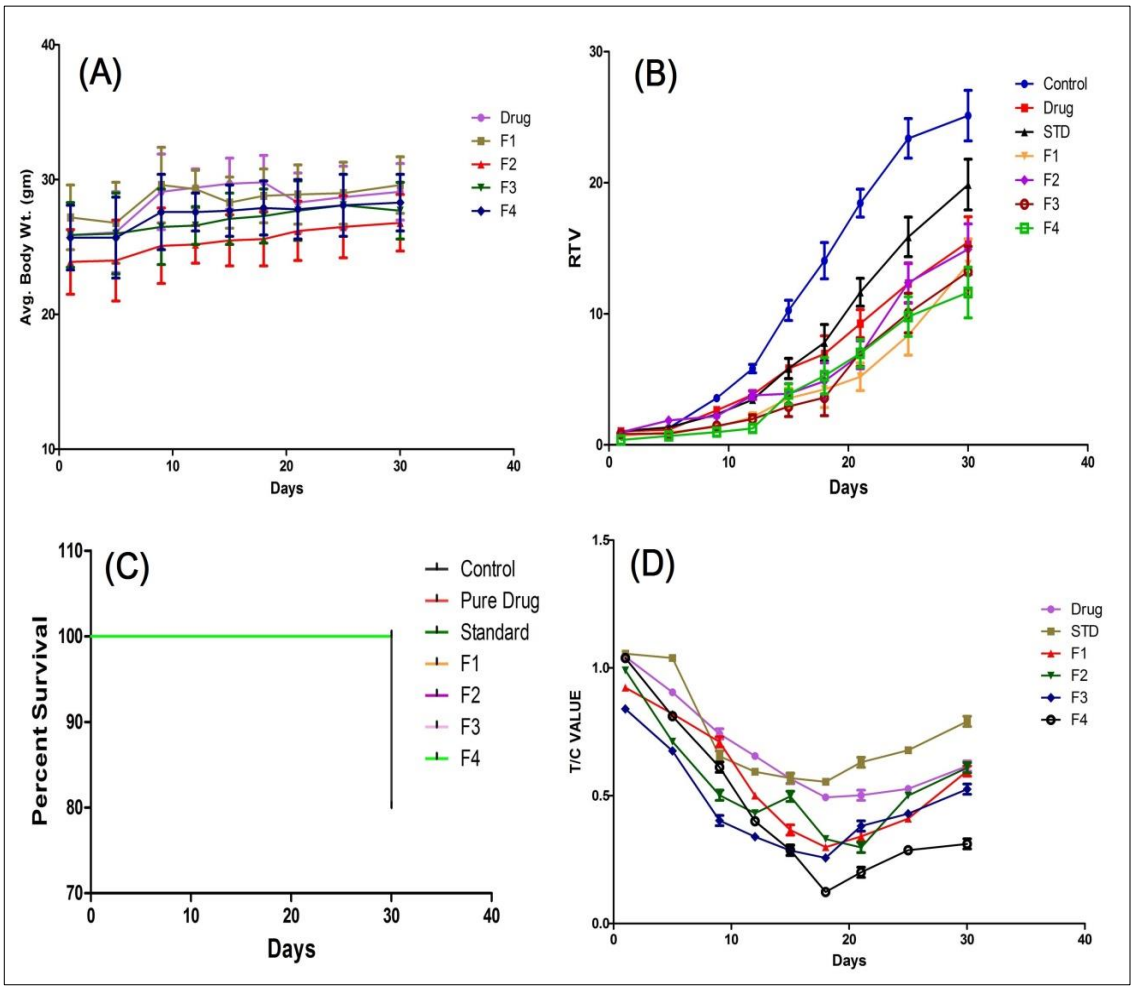

Figure 5.39 (A) Average body weight (g) of mouse mammary tumor model C3H/J altered with respect to number of days; (B) Relative tumor volume data curve of mouse mammary tumor model of control, pure drug, standard (STD) and optimized formulations (25 mg/Kg i.v. weekly x 4 weeks) from day 1 to 30; (C) Survival data (%) using Kaplan-Meier curve of mouse bearing mammary tumor model treated with all seven treatment groups by log-rank test; (D) T/C values from RTV data of mouse mammary tumor model C3H/J demonstrated significant activity of optimized formulations

(Vertical bars represent SEM; n=6)

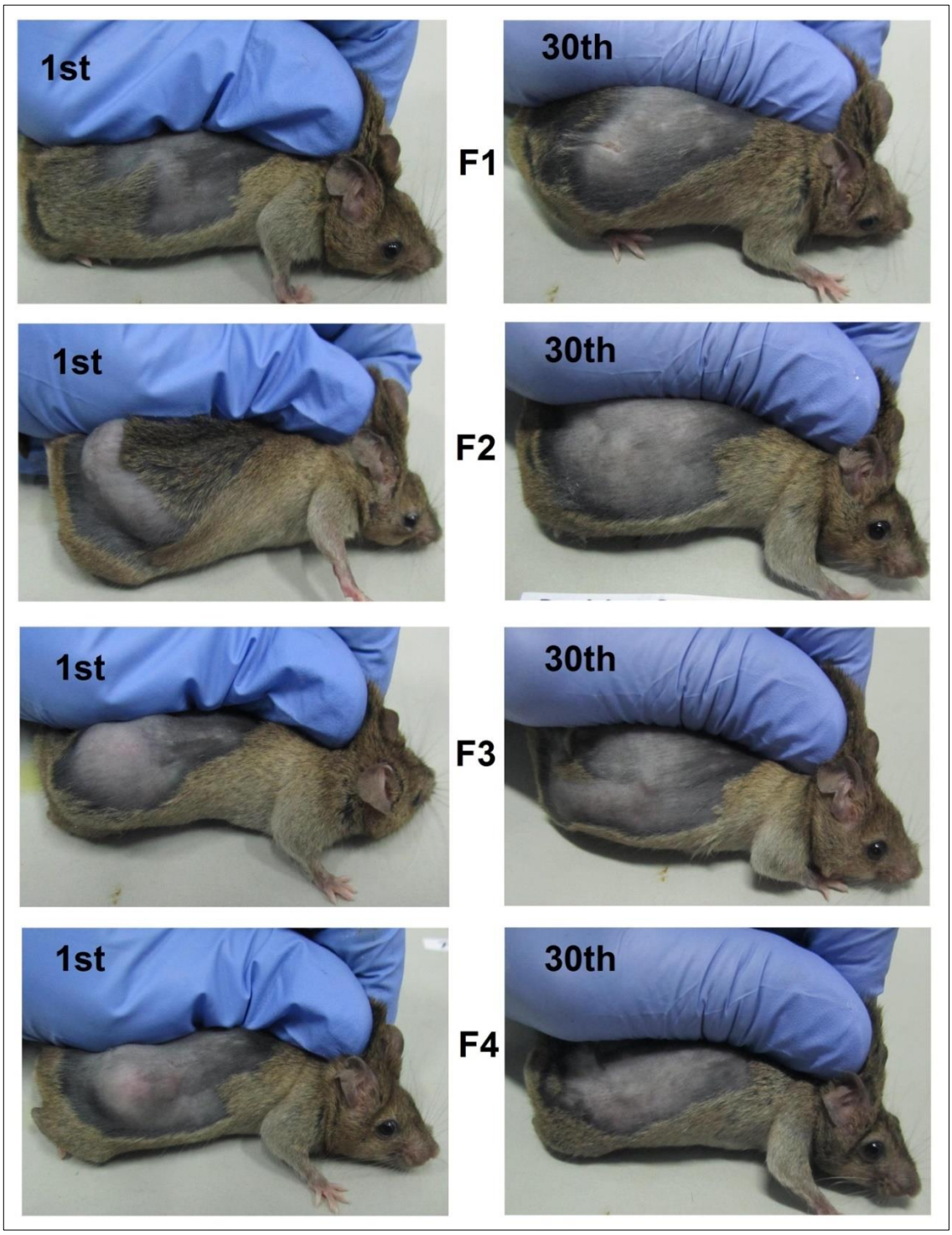

Figure 5.40 Photographs representing tumor bearing mice on first and last days of treatment with the optimized formulations

5.13 Stability studies

As per ICH guideline Q1A (R2), the accelerated stability studies were carried out over a period of 6 months at 40±2°C, 75±5% RH [Guideline, 2003]. The results of stability studies are shown in Figure 5.41. Particle size increased marginally while zeta potential and entrapment efficiency decreased over time during 6 months storage may be due to high aggregation and agglomeration tendencies. The findings through F1, F2, F3 and F4 values were statistically significant (p<0.05) indicating stability for all the prepared batches of nanoformulation.

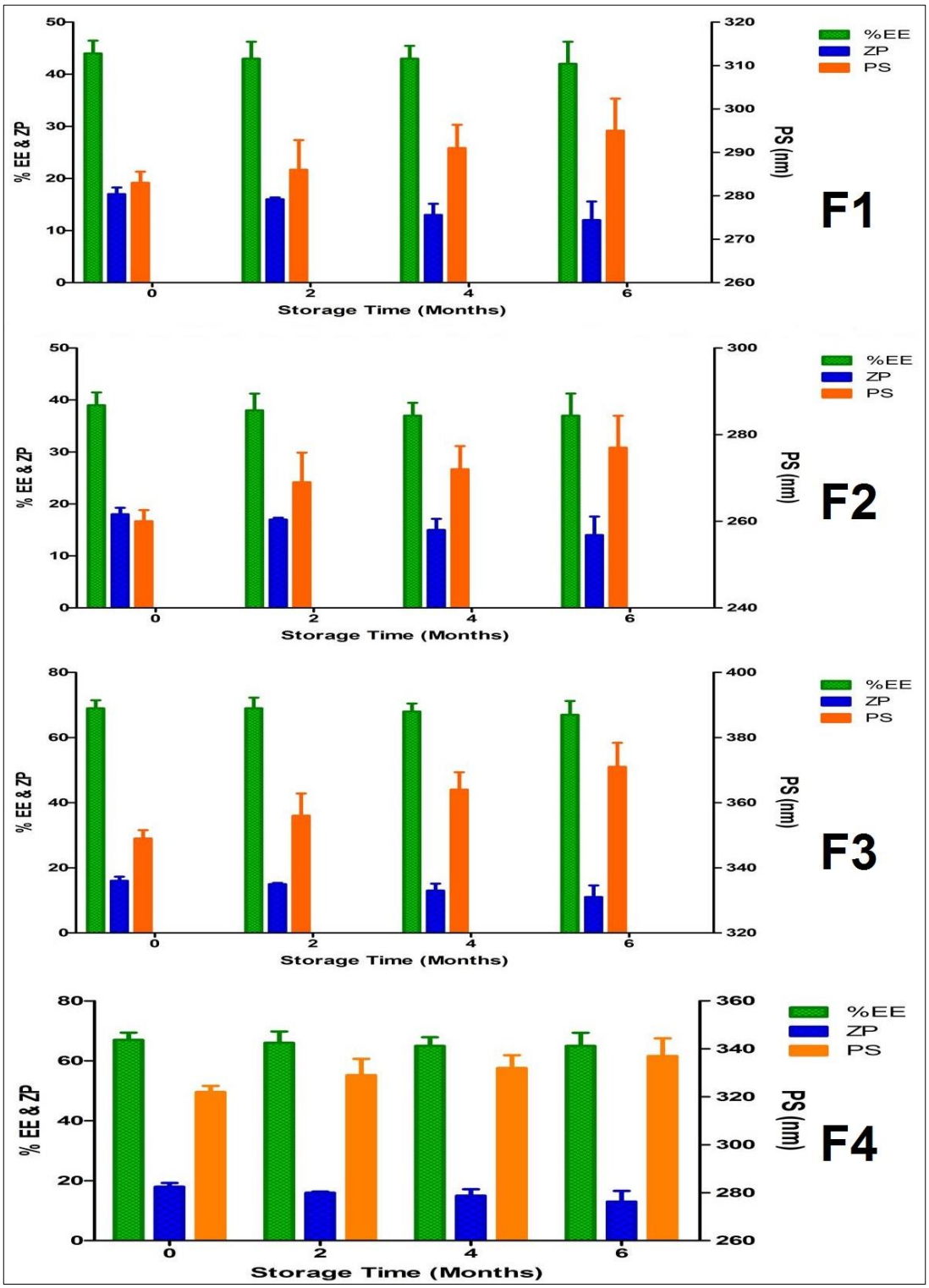

Figure 5.41 Stability profile for particle size, zeta potential and % entrapment efficiency for 6 months' storage period (vertical bars represent SEM; n=3)